

Validation of Metop PMAp a  
products using AATSR Aerosol  
CCI data and the ECHAM Model  
Data

Final report

Caroline Poulsen and Nick Schutgens\*

\*University of Oxford



*Report prepared by*

*RAL Space*

*Remote Sensing Group*

*Harwell Oxford*

*Chilton, OX11 0QX*

*United Kingdom*

*In response to*

*EUMETSAT ITT*

*13/207655*

*2015-08-24*



**RAL Space**  
STFC Rutherford Appleton Laboratory,  
Harwell Oxford,  
Didcot,  
OX11 0QX UK  
[www.stfc.ac.uk/RALSpace](http://www.stfc.ac.uk/RALSpace)

Document: Final Report

Customer Ref: ITT 13/207655

RAL Space Ref: SSTD1628

2015-08-24

Page 1 of 66

## CONTENTS

FINAL REPORT .....	3
Acronyms Used in this REPORT .....	3
1. Validation of PMAP with ECHAM model data .....	4
1.1. Overview .....	4
1.2. Description of PMAp Algorithm and data .....	5
1.3. AATSR ORAC AEROSOL CCI data.....	6
1.4. The ECHAM Model .....	9
1.5. Collocation of data .....	12
2. APPROACH TO THE STUDY.....	13
2.1. Benefits of model-satellite comparison .....	13
3. RESULTS .....	16
3.1. General Analysis Approach .....	16
3.2. Global look At ECHAM DATA.....	18
3.3. Results of June/July 2013 METOP-A and METOP-B Comparison .....	21
3.4. Regional Analysis.....	27
3.5. Results of June 2010 Metop-A and AATSR Comparison.....	40
3.5.1. Detailed discussion on Differences between model and satellite biomass burning .....	41
3.6. Comparison with Aeronet Data.....	52
3.7. Results of Case Study: Large European dust event March/April 2014.....	53
4. CONCLUSIONS.....	58
4.1. Further work and reccomendations.....	60
5. References .....	62

## FINAL REPORT

### ACRONYMS USED IN THIS REPORT

Table 1: List of acronyms used in this report

RAL	Rutherford Appleton Laboratory
RSG	Remote Sensing Group
STFC	Science and Technology Facilities Council
EO	Earth Observation
AOD	Aerosol Optical Depth
AAI	Aerosol Absorbing Index
OU	Oxford University
MACC	Monitoring of Atmospheric Composition and Climate
ECHAM	European Centre for medium range weather forecasting HAMBURG (Climate Model developed at Max Planck Institute for Meteorology)
MAN	Maritime Aerosol Network
ORAC	Optimal retrieval of Aerosol and Cloud
CCI	Climate Change Initiative
ECMWF	European Centre for Medium Range Weather Forecast
BADC	British Atmospheric Data Centre
CEDA	Centre for Environmental Data Archive
CIS	Community Intercomparison Suite
NWP	Numerical Weather Prediction

## 1. VALIDATION OF PMAP WITH ECHAM MODEL DATA

### 1.1. OVERVIEW

The aim of this study is to validate the Metop PMAp products with modelled AOD values produced by a general circulation transport model that includes realistic aerosol dynamics and partitioning schemes and uses realistic background meteorology and transport information. The model selected that satisfied this criterion was the ECHAM-HAM model. The MACC model was considered however the MACC model assimilates satellite data which could have biased the comparison. The satellite data was compared for 4 months: July 2010, June and July 2013 and a month selected to cover the extreme Saharan dust events over Europe in March/April 2014. Table 2 summarises the data sets analysed. The following sections include short descriptions of the data sets and model, the used collocation tools and the results of the Intercomparison. Finally at the end of the report we summarise the results in the conclusion and provide some further recommendations.

Date	PMAp Data	ECHAM	Aeronet
July 2010	Full month	Full month	Full month
June 2013	Full month	Full month	Full month
July 2013	Full month	Full month	Full month
March 2014	22 <sup>nd</sup> -31 <sup>st</sup>	22 <sup>nd</sup> -31 <sup>st</sup>	22 <sup>nd</sup> -31 <sup>st</sup>
April 2014	1 <sup>st</sup> -5 <sup>th</sup>	1 <sup>st</sup> -5 <sup>th</sup>	1 <sup>st</sup> -5 <sup>th</sup>

Table 2: Table showing the data considered in this study

## 1.2. DESCRIPTION OF PMAp ALGORITHM AND DATA

The PMAp algorithm is configured as a multi-instrument, but single platform aerosol retrieval algorithm. PMAp currently uses AVHRR/3 and GOME on Metop-A and Metop-B. IASI is already technically integrated into the PPF and is planned to be used in further releases.

The AVHRR/3 is a six-channel scanning radiometer providing three solar channels in the visible/near-infrared region and three thermal infrared channels with spatial resolutions up to 1.1 km. GOME-2 is a medium-resolution double UV-VIS spectrometer, fed by a scan mirror which enables across-track scanning in nadir, as well as sideways viewing for polar coverage and instrument characterisation measurements using the moon. The PMAp algorithm uses the so-called Polarization Monitoring Devices (PMD) which provides reflectance's and stokes fraction in 16 different bands ranging from the UV to the red edge (311 nm – 805 nm).

The multi-sensor PMAp product is produced as GOME-2 product with the spatial resolution of the GOME-2 PMD footprint see Table 3.

Satellite Platform	Spatial resolution (GOME-2 resolution)	Swath
Metop-A	5x40km	960km
Metop-B	10x40km	1920km
Metop-C	TBD	TBD

**Table 3 Satellite platform and resolution and swath of PMAp products**

If we use only Metop-A data, we get global coverage for the chosen latitudes (from +70 to –70) over approximately three days. If we use only Metop-B data, we get global coverage at these altitudes over approximately 1.5 days. Using the two instruments in tandem, we get daily global coverage. The PMAp AOD product does have some gaps in coverage. This is due to thick clouds and problematic observation geometries (sun glint conditions), depending on the conditions of the measurements. In summary, we expect a typical global AOD coverage of about 3-4 days using Metop-A/Metop-B tandem operations, as opposed to one week using only Metop-B and two weeks using only Metop-A.

The algorithm consists of three steps:

Step 1: A pre-classification is applied based on AVHRR. This includes the detection of clouds, calculation of cloud correction factors, detection of strong dust and ash events as well as a pre-classification of possible aerosol types.

Step 2: A set of up to 28 AODs and up to 28 chlorophyll corrections are retrieved. Each of these AODs is retrieved with respect to a different aerosol type. An unknown in the algorithm is exactly which aerosol type is

the best representation of the given scene. This is simplified for partly cloudy pixels and specific observation geometries

Step 3: One of the 28 models is selected–this is the one which best fits the satellite measurements. [REF14]

### 1.3. AATSR ORAC AEROSOL CCI DATA

Applied to Advanced Along Track Scanning Radiometer (AATSR) measurements in the Aerosol\_cci project, ORAC is a dual-view aerosol retrieval scheme for use over both land and ocean surfaces (Thomas et al., 2009). ORAC retrieves aerosol optical depth and effective radius, as well as the surface reflectance at each of the four AATSR short-wave channels, using a mixture of pre-defined aerosol components. The algorithm has also been shown to have limited skill at selecting aerosol type from a range of possibilities (represented by differing mixtures of aerosol components).

ORAC is built around the optimal-estimation retrieval formulism, and thus provides full uncertainty propagation (from estimates of measurement noise, forward model uncertainty and a priori constraint), the ability to apply a priori constraints in a mathematically rigorous and consistent way, and extensive retrieval statistics and diagnostics.

In the configuration used for aerosol\_cci, ORAC uses the first four (A)AATSR channels (i.e. 0.55, 0.67, 0.87, 1.6  $\mu\text{m}$ ) in both views.

The parameters retrieved by ORAC are:

- The log<sub>10</sub> of aerosol optical depth (AOD) at 0.55  $\mu\text{m}$ .
- The log<sub>10</sub> of aerosol effective radius (in units of log<sub>10</sub>( $\mu\text{m}$ ))
- Surface bi-hemispheric reflectance at each measurement wavelength.

In addition, the product includes AOD at 0.67, 0.87 and 1.6  $\mu\text{m}$ , as well as the fine-mode AOD, dust AOD and absorbing AOD, all at 0.55  $\mu\text{m}$ . These parameters are not directly retrieved, but are computed based on the properties of the aerosol model used in the retrieval.

The retrieval is run using 10 different aerosol microphysical models, which in turn are made up of mixtures of four standard aerosol components that are used for all aerosol cci products. These four components are broadly defined as follows:

- Weakly absorbing fine mode aerosol
- Strongly absorbing fine mode aerosol
- Desert dust (coarse mode)
- Sea salt (coarse mode)

A detailed description of the aerosol components is given by Holzer Popp et al. (2014). It should be noted that the retrieval of aerosol effective radius is equivalent to retrieving the fine mode fraction, as the effective radius is changed by altering the mixing ratio of the fine and coarse mode components within each aerosol

model. The “best” aerosol model is chosen for each retrieval pixel *a posteriori* using two different approaches, which provide two separate product versions:

v03.02: The aerosol model which provides the best fit to the measurements is chosen.

V03.04: The AEROCOM climatology of aerosol type, compiled by Steffan Kinne, is used to constrain the aerosol model chosen. If an aerosol model consistent with the climatological prediction provides a good fit to the measurements, then it is chosen, in preference to other models which provide good (or better) fits.

Cloud cleared reflectance data is averaged onto a 10 km sinusoidal grid prior to retrieval (the grid is actually specified as having 4008 cells around the equator, which is the closest integer number to a 10 km spacing). For aerosol\_cci, data is supplied in NetCDF files, following the CF-1.6 naming conventions.

In these files the log10 values have been converted to a linear scale, i.e. the files contain aerosol optical depth and effective radius. The uncertainty on these values is expressed as  $\log_e(10)\delta\log_{10}(x)x$ , where  $x$  is the retrieved value transformed into linear space (optical depth or effective radius) and  $\delta\log_{10}(x)$  is the uncertainty on the log10 value of  $x$ . Thus, the uncertainties provided on optical depth and effective radius do not directly correspond to the one standard deviation interval about the retrieved state, but are representative.

The ORAC aerosol product is still undergoing evaluation within the aerosol\_cci project, thus detailed validation results are not yet available. Initial comparisons show that both versions of the product provide accurate global AOD, with correlations between 0.7 and 0.8 with AERONET sun photometer measurements.

Figure 1 shows the global AOD at 550nm for the ORAC Aerosol retrieval. Figure 2 Shows an Aeronet Comparison for the whole time period showing excellent correlation over sea and land.

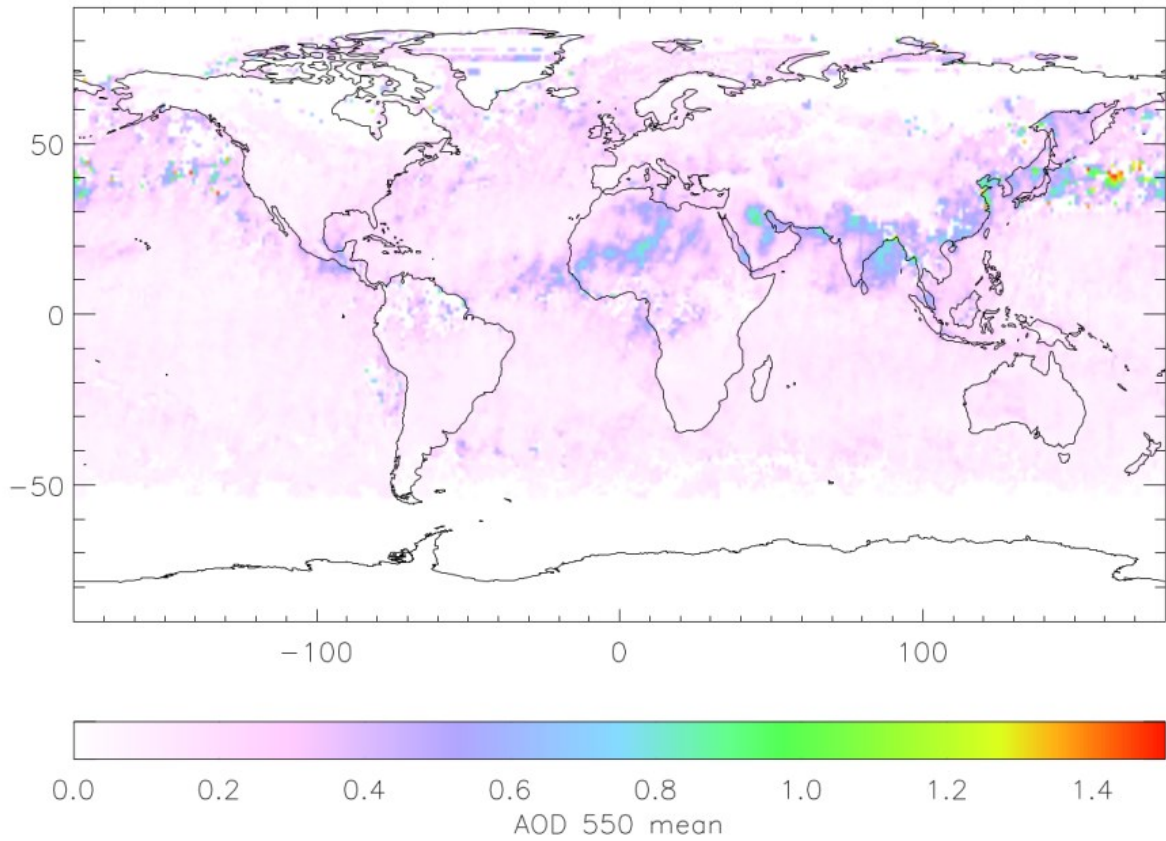


Figure 1 Global AOD at 550nm from the ORAC AATSR retrieval

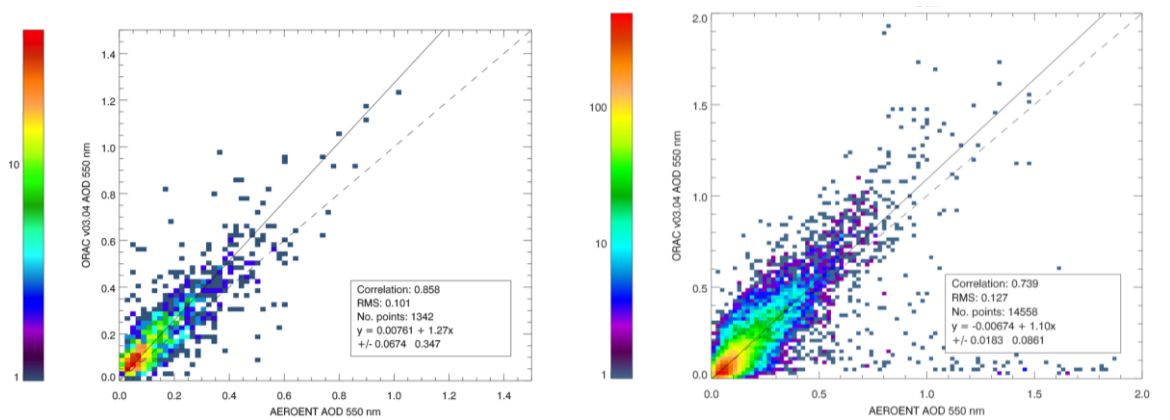


Figure 2 Comparison of AATSR ORAC AOD and 550nm with Aeronet observations, over sea, left and over land ,right

## 1.4. THE ECHAM MODEL

The global aerosol model ECHAM-HAM consists of an aerosol module HAM (Stier et al. 2005a, Stier et al. 2007a) coupled to an atmospheric general circulation model ECHAM (Roeckner et al. 2003a, Roeckner et al. 2006a). ECHAM-HAM has been used to study non-linearities in aerosol response due to emission changes (Stier et al. 2006a), aerosol effects in a transient climate (Stier et al. 2006b), aerosol activation and cloud-processing (Roelofs et al. 2006a), aerosol indirect effects (Lohmann et al. 2007a), the impact of pollution mitigation on climate forcing (Kloster et al. 2008a), the impact of volcanic eruptions on climate (Niemeier et al. 2009a, Timmreck et al. 2010a), the impact of aerosol nucleation on radiative forcing (Makkonen et al. 2009a, Kazil et al. 2010a), dimming and brightening of surface radiation due to aerosols (Follini et al. 2011a), climate forcing due to secondary organic aerosols (O'Donnell et al. 2011a) and aerosol indirect effects due to shipping emissions (Peters et al. 2012a) to name but a few studies.

The general circulation model ECHAM was developed at the Max Planck Institute for Meteorology and evolved from the model at the European Centre for Medium-Range Weather Forecasting. It solves the prognostic equations for vorticity, divergence, surface pressure and temperature using spherical harmonics with triangular truncation. Tracers like water vapour, liquid and ice hydrometeors, various trace gases as well as aerosols are advected with a flux-form semi-Lagrangian transport scheme (Lin et al. 1996a) on a Gaussian grid. ECHAM can be nudged to meteorological reanalysis fields. More details can be found in Roeckner et al. 2003a, 2006a.

The aerosol module HAM calculates the global evolution of five aerosol species: sulfate ( $\text{SO}_4$ ), particulate organic matter (POM), black carbon (BC), sea salt (SS) and dust (DU). These species are the constituents of both internally and externally mixed aerosol particles whose size distribution is represented by 7 uni-modal log-normal distributions called modes. These 7 modes describe four size classes (nucleation, Aitken, accumulation and coarse) and two hygroscopic classes (hydrophobic and hydrophilic). Most of these modes contain time- and space-varying mixtures of aerosol species. To predict aerosol evolution, ECHAM-HAM (without explicit SOA, see later) uses 25 tracers: 7 for number mixing ratios and 18 for mass mixing ratios.  $\text{H}_2\text{SO}_4$  nucleation & condensation, coagulation and ageing are handled by the M7 sub-module by Vignati et al. 2004a. The processes described in M7 cause redistribution of aerosol mass and numbers among the modes. Part of HAM is a sulphur cycle model (Feichter et al. 1996a) that predicts the evolution of dimethyl sulphide (DMS), sulphur dioxide ( $\text{SO}_2$ ) and gaseous sulfate ( $\text{SO}_4$ ) using monthly mean fields of the oxidants OH,  $\text{H}_2\text{O}_2$ ,  $\text{NO}_2$  and  $\text{O}_3$ , calculated off-line by the MOZART chemical transport model (Horowitz et al. 2003a). The aerosol in HAM is affected by the meteorology calculated by ECHAM, and in turn provides feedback to ECHAM as it affects atmospheric radiative transfer and cloud microphysics.

Over time, various improvements have been made to ECHAM-HAM and currently a distinction is made between the initial version HAM 1 (Stier et al. 2005a) and the newer version HAM 2 (Zhang et al. 2012a). While using the same modal structure, HAM 2 added new parametrisations for nucleation, sea salt and dust emissions, a water uptake scheme based on  $\kappa$ -Kohler theory and an explicit scheme for secondary organic aerosol (SOA) formation. For a detailed overview of the differences between HAM 1 and HAM 2, see Zhang et al. 2012a, who also define the default choices for an ECHAM-HAM experiment.

In this paper, we will use ECHAM6-HAM2, nudged to ERA-interim meteorological reanalysis. Emissions are based on either parametrisations for dust and sea-salt or inventories for POM, BC and SO<sub>2</sub>. The emission of dust is based on wind-speeds and soil moisture as well as a map of identified preferential dust sources. Sea-salt emissions are based on wind-speeds. The inventories are combinations monthly averaged inventories (ACCMIP/MACcity) for anthropogenic emissions (e.g. due to industry, transport, agriculture) or daily emissions due to wildfires (GFAS). To reduce the complexity of the analysis, we chose to use the implicit SOA modelling scheme from HAM 1 instead of the explicit scheme that was introduced with HAM 2. For computational reasons, the implicit scheme is currently considered the default option. It assumes that a specified fraction (65%) of biogenic emissions are soluble and directly condense onto pre-existing hydrophilic aerosol. Thus particle growth through condensation of volatile gases is considered albeit in an abstract fashion. Over land, this condensation often dominates primary emissions into the hydrophobic Aitken and accumulation modes but it seldom dominates as a source of total aerosol mass in those modes

ECHAM-HAM has been extensively evaluated and contributes to the full set of AeroCom model intercomparison studies ([www.aerocom.met.no](http://www.aerocom.met.no)). The ECHAM model is typically run at T63 (approx. 1.8 degrees) resolution but for short periods of time (i.e 1 month) can be run at T106 (approx. 1 degree) resolution. In this study, the ECHAM meteorology was nudged to the ERA interim reanalysis to ensure the best representation of atmospheric flows.

For the purposes of the current project, ECHAM-HAM is run at T63 resolution (1.8 degree gridboxes) with 31 levels in the troposphere and lowest stratosphere. Wildfire emission inventories are for the relevant time frame, but anthropogenic emission inventories are for 2010. We do not expect much change in the latter inventories over a few years.

Below we discuss an evaluation of ECHAM-HAM with remote sensing data. The model was run for 2007 with appropriate emissions and nudged to the ECMWF ERA interim reanalysis. The following remote sensing datasets were used as part of the evaluation:

1. MODIS Aqua AOT as delivered by NRL
2. AERONET Direct Sun level 2 AOT and AE

In all cases, model data has first been collocated in time and space with available observations before any comparison was made. Still, it's important to point out there is a big discrepancy in the spatial aggregation of model and observational data: while grid-boxes on the equator are ~ 200 by 200 km in size, field-of-view of many observations is only ~10 km (nominal MODIS pixel size) or less. This in itself introduces differences between model values and observations that are substantial (i.e. larger than retrieval errors) and necessitate further spatial and/or temporal averaging of the data before comparison.

In Figure 3, we show the difference between yearly averaged model AOT and MODIS Aqua AOT. A very general pattern is the underestimates by the model over land and overestimates over ocean. Even so, large parts of both the land and ocean show rather small deviations of the modelled AOT from observations.

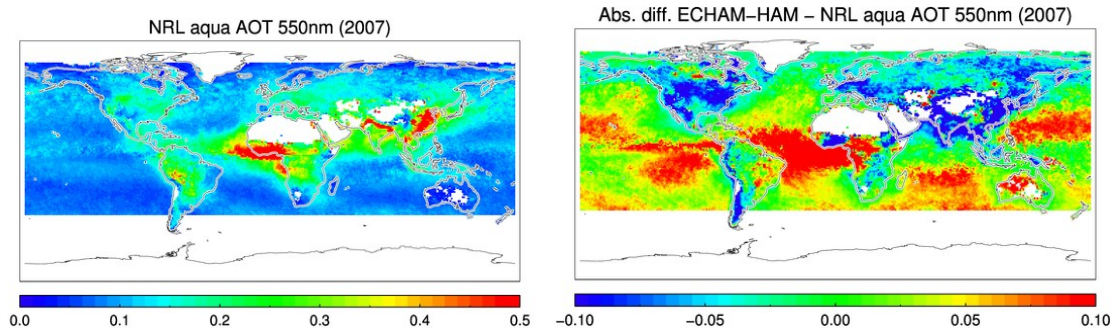


Figure 3 On the left, yearly averaged MODIS Aqua AOT; on the right the difference between modelled and observed AOT

Comparing yearly averaged modelled AOT with AERONET, the patterns of over- and underestimation agree broadly with the satellite comparison (not shown).

In particular, the model does pretty well in modelling AE, as shown in Figure 4. AE may be interpreted as an indication of particle size and, indirectly, a first clue to a particles speciation.

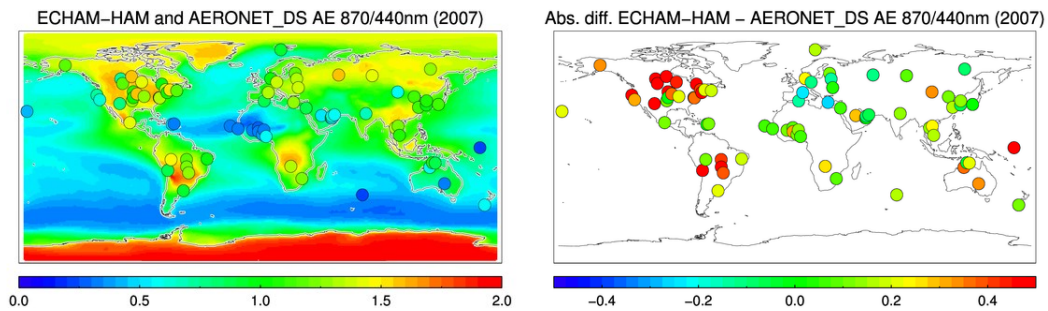
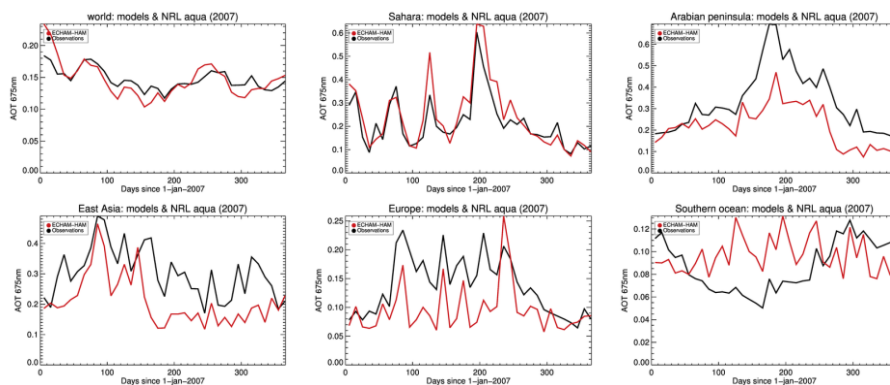
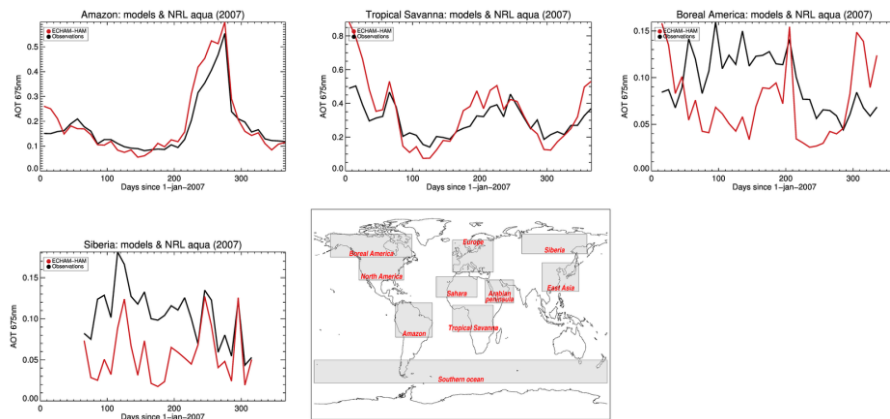


Figure 4 On the left, yearly averaged modelled and AERONET observed AE; on the right the difference

Finally, in Figure 5 we show time-series of model and Aqua AOT, when averaging the observations over large regions and 10 days. These graphs strongly bring out regions where the model performs either poorly or well.





**Figure 5 Time-series of modelled and MODIS Aqua AOT for different regions**

We see that the model does quite well in a global sense, but has issues over in particular air pollution regions (Europe and East Asia) as well as the southern ocean. In contrast, dust storms, especially those from Africa, are represented very well and so are biomass burning events in the Amazon and over the tropical Savannah.

Very briefly, we'd like to provide *possible* explanations for some of the discrepancies we see between model and observations. Although not shown here, time-series of AERONET AOT in general bear out the results for MODIS AOT, so retrieval errors are unlikely to be the main cause. Of all dust regions, Northern Africa has been studied the best and sophisticated dust models exist for this region. In comparison, the Saudi-Arabian peninsula has received far less scrutiny. The complex processes that contribute to dust emission imply that dust emissions parametrised in models are strongly tuned. Over polluted areas (Europe and East-Asia), the model AOT is always too low although there is a strong temporal correlation between model and observations. The underestimation is likely due to the absence of nitrate as aerosol in the model and the rather unsophisticated treatment of VOCs (Volatile Organic Compounds) and their resulting SOA (Secondary Organic Aerosol). Finally, biomass burning events (or wild-fires) depend strongly on proper emission inventories which are themselves derived from satellite observations. It seems reasonable to assume that large emissions are caused by large fires that are easily observed from space. The different AOT levels for Amazon and the Savannah compared to Boreal America and Siberia suggest remaining issues with the satellite emission inventories.

## 1.5. COLLOCATION OF DATA

**The Community Intercomparison Suite (CIS)** is an automated model/data intercomparison tool simplifying a wide range of time-consuming tasks in intercomparison (read-in of heterogeneous gridded and ungridded model data and observations, reduction, co-location, and analysis) to a set of simple commands. CIS can handle both observational datasets (e.g. remote sensing like AERONET sun photometers, MODIS and MISR satellite imagers, the space born lidar CALIOP and radar CloudSAT and ESA Climate Change Initiative data or in-

situ data, such as the largest archive of aircraft measurements of aerosol collected in the NERC project GASSP) as well as global models, such as ECHAM or AeroCom models used in this project. The collocation tool in CIS allows selection of user specified collocation kernels (e.g. interpolation, nearest neighbours) and is being optimised for efficiency for the handling of large datasets). Deployed in the JASMIN data super cluster at CEDA, CIS was used as technical framework for this study.

This tool is developed as open source, written in Python, so is available to EUMETSAT to rerun or modify after the study is complete.

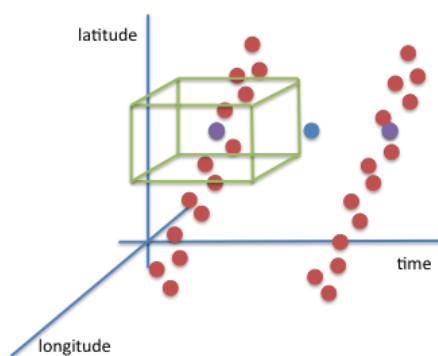


Figure 6: Illustration of the collocation feature of CIS. Satellite overpasses (red) are sampled at AERONET sunphotometer locations (blue and purple) with a user specified collocation criteria in space-time (green box). This is achieved with a single command line: `CIS col <destination sampling> <variable>:<source file>:<collocation method> -o <output file>`.

The collocation of the satellite and model data was performed with the CIS tool described above. The CIS tool can currently read in netcdf and hdf data. A key advantage of the CIS tool is its applicability to multiple data sets, including standard netCDF-CF model output, a wide range of satellite datasets, and the minimal effort required to switch data sources; hence future comparisons with the same data sets or different data sets could be simply implemented.

A 'plugin' was written in python to read the PMAP, SEVIRI, Aeronet and AATSR data and collocations of satellite data performed. The collocated data sets are stored as Net CDF files and can be made available to EUMETSAT on request.

More information and how to use CIS can be found at <http://jasmin-cis.readthedocs.org/en/latest/#>

Plugins can be found at <http://www.cistools.net>

## 2. APPROACH TO THE STUDY

### 2.1. BENEFITS OF MODEL-SATELLITE COMPARISON

Conventional satellite retrieval validation has focussed on validating retrievals with Aeronet observations. The advantage of this technique is that Aeronet observations have a high accuracy and hence the interpretation of the accuracy of satellite retrievals in clear scenes collocated with Aeronet sites is relatively straight forward however there are some clear disadvantages to this technique. Aeronet observations have sparse coverage over land and very poor coverage via the MAN (Maritime Aerosol Network) over sea, which while informative

cannot provide a robust statistical analysis and certainly not in partly cloudy scenes which is what is required here.

Satellite observations have typically been used to validate model simulations. This has been an important task within the AeroCom community as only satellite data can provide continuous global coverage of aerosols. On the other hand the satellite observations have significant limitations. Because of the small information content in the satellite radiances, satellite retrievals typically have limited information on aerosol speciation and particle size, an area where microphysical aerosol models, such as ECHAM-HAM, can provide physically realistic constraints.

Satellite retrievals may also have difficulty distinguishing high aerosol loadings from cloud and hence in forming a consistent data set may remove significant aerosol events with high aerosol loadings in order to reduce cloud contamination globally.

Similarly very thin clouds maybe mistaken as aerosols, by ground based and satellite instruments. Thus the detailed analysis as proposed here would gain insight into the efficiency of the cloud screening.

For aerosols the most common satellite product is column AOD whereas the model has the full 3D distribution of the aerosol microphysical state, i.e. composition, size and mixing state from which physically consistent AOD is calculated. This information can be used to improve the satellite retrieval either through detailed analysis and the more appropriate selection of aerosol model used in the retrieval and/or the use of model information as apriori information in the retrieval.

In summary model data can make a valuable contribution to evaluating satellite data particularly where ground based validation is sparse e.g. over the sea, where the likelihood of flagging high aerosol loading is high and for aiding the attribution of differences between ground based validation or model comparisons to the 3D structure of the aerosol and the composition.

Region	Latitude range	Longitude range
China:	10-50	90-150
India	0-30	60-90
North Atlantic	30-75	150—100
North Pacific	30-75	150—100
Saharan West Coast	0-30	-40-0
Saharan West Coast close	6-30	-20-0
Saharan West Coast far	6-30	-40—20

Sahara East coast	0-45	15-65
Southern Africa	-30-10	-20-20
Southern Africa1(Angola/Congo)	-30 --5	-20-20
Southern Africa2(Sahel)	-5-10	-20-20
South Atlantic	-75--10	-60-25
Southern Indian Ocean	-70--10	30-110
South Pacific Ocean	-80--50	-180-180
Tropics	-20-20	-180—110

Table 4: Table showing regions for which results were analysed.

### 3. RESULTS

The results of this study are presented in 4 sections

1. Comparison of June and July 2013 METOP-A and METOP-B PMAp retrievals with ECHAM data
2. Comparison of July 2010 METOP-A PMAp retrievals with ECHAM and a corresponding AATSR/ECHAM comparison with ORAC AATSR Aerosol CCI retrievals.
3. Case study European dust event March/April 2014
4. Comparison with Aeronet

#### 3.1. GENERAL ANALYSIS APPROACH

1. Satellite Data is collocated at L2 with ECHAM model data using the CIS tools.
  - a. The PMAp version is 1.010
    - i. A previous version of PMAp was analysed prior to this latest release. The comparison with model data revealed cloud contamination in some coastal stratocumulus regions which is improved in the latest release.
  - b. The ECHAM version is ECHAM6-HAM2
    - i. The data is provided at 3 hourly temporal resolution
    - ii. 1.8 degree resolution (200 km at the equator)
2. Results are presented as:
  - a. Global and regional maps: The regions are selected so as to focus on the skill of retrieving distinct aerosol scenarios such as desert dust, maritime and biomass burning aerosol types.
  - b. Time series of aerosol optical depth, single scattering albedo and composition.
  - c. Scatter plots of model vs satellite AOD. The scatter plots are an accumulation of the level2 collocated swaths.

Variable	Abbreviation
Aerosol Optical Depth	AOD
Single Scattering Albedo	SSA
Composition	DU: Dust SO4: Sulphate SS: Sea Salt OC: Organic carbon BC: Black Carbon



**RAL Space**  
STFC Rutherford Appleton Laboratory,  
Harwell Oxford,  
Didcot,  
OX11 0QX UK  
[www.stfc.ac.uk/RALSpace](http://www.stfc.ac.uk/RALSpace)

Document: Final Report	
Customer Ref: ITT 13/207655	
RAL Space Ref: SSTD1628	
2015-08-24	Page 17 of 66

	WAT: Water
AE	Angstrom coefficient

**Table 5 Model variables and associated abbreviations**

AOD is the most direct comparison one can perform with the model. The auxiliary model information is included to provide key insights. The SSA indicates how absorbing or scattering the Aerosol was, the Angstrom coefficient gives an idea of the size of the particles and the column burdens what type of aerosol is in the model. Note that the column burden is not linearly correlated to the AOD but gives a good indication of the major aerosol species potentially being observed by the satellite.

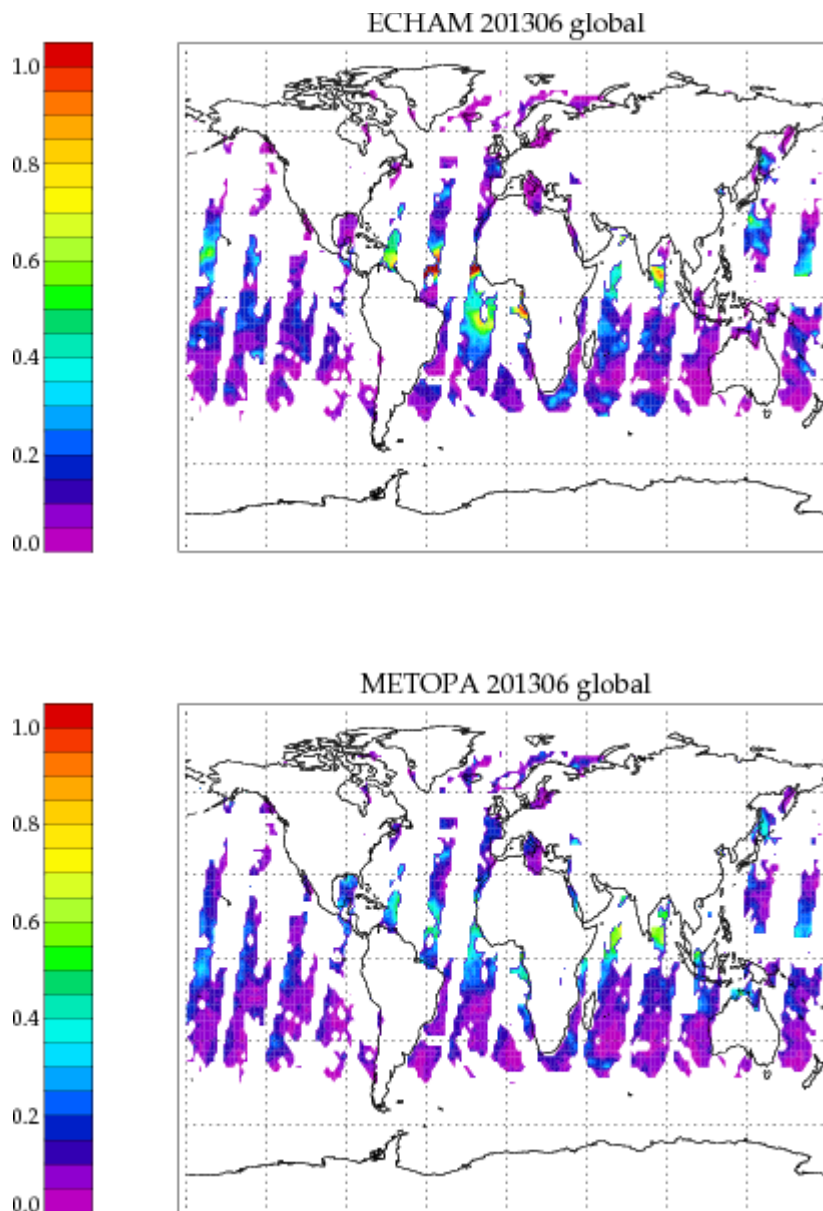


Figure 7 Example of collocated model (top) and satellite (bottom) swaths for a single day, 15th June 2013.

### 3.2. GLOBAL LOOK AT ECHAM DATA

Figure 8 shows maps of the parameters contained in the model data. The model data produces diagnostics on model levels, and for comparison to the satellite data a total column value is calculated.

The top left plot shows the single scattering albedo. The single scattering albedo is a measure of the effectiveness of scattering relative to extinction for the light encountering the atmospheric aerosol particles. It is a dimensionless quantity and ranges from 0 to 1. The value is 1 for purely scattering aerosol (e.g. seasalt) and below 1 when absorbing aerosols are present e.g. biomass burning aerosol.

The following plots show the aerosol burden the burden is defined as the atmospheric column-integrated mass of a particular aerosol species (dry, i.e. without the contribution of condensed water). Note that a particular aerosol species may be present in several modes and may be mixed with other species. For the calculation of burden this is irrelevant. Burdens are usually given in  $\text{kg/m}^2$ .

The bottom right plot shows the Angstrom coefficient defined as the exponent that expresses the spectral dependence of aerosol optical thickness ( $\tau$ ) with the wavelength of incident light ( $\lambda$ ). The Angstrom exponent provides additional information on the particle size (the larger the exponent, the smaller the particle size), aerosol phase function and the relative magnitude of aerosol radiances at different wavelengths. Typically you see low values for large particles such as desert dust and higher values for continental type aerosols.

The importance of sampling the model as a function of swath is illustrated in Figure 9 which shows the ECHAM data average over a single month for all values and bottom the ECHAM data sampled with the PMAp swath. While the overall spatial pattern remains the same significant differences are apparent that we shall see in the analysis to follow can be greater than the difference between the satellite and model. Without sampling the model it would be difficult to attribute the biases to differences in sampling (spatial and temporal) or actual physical differences.

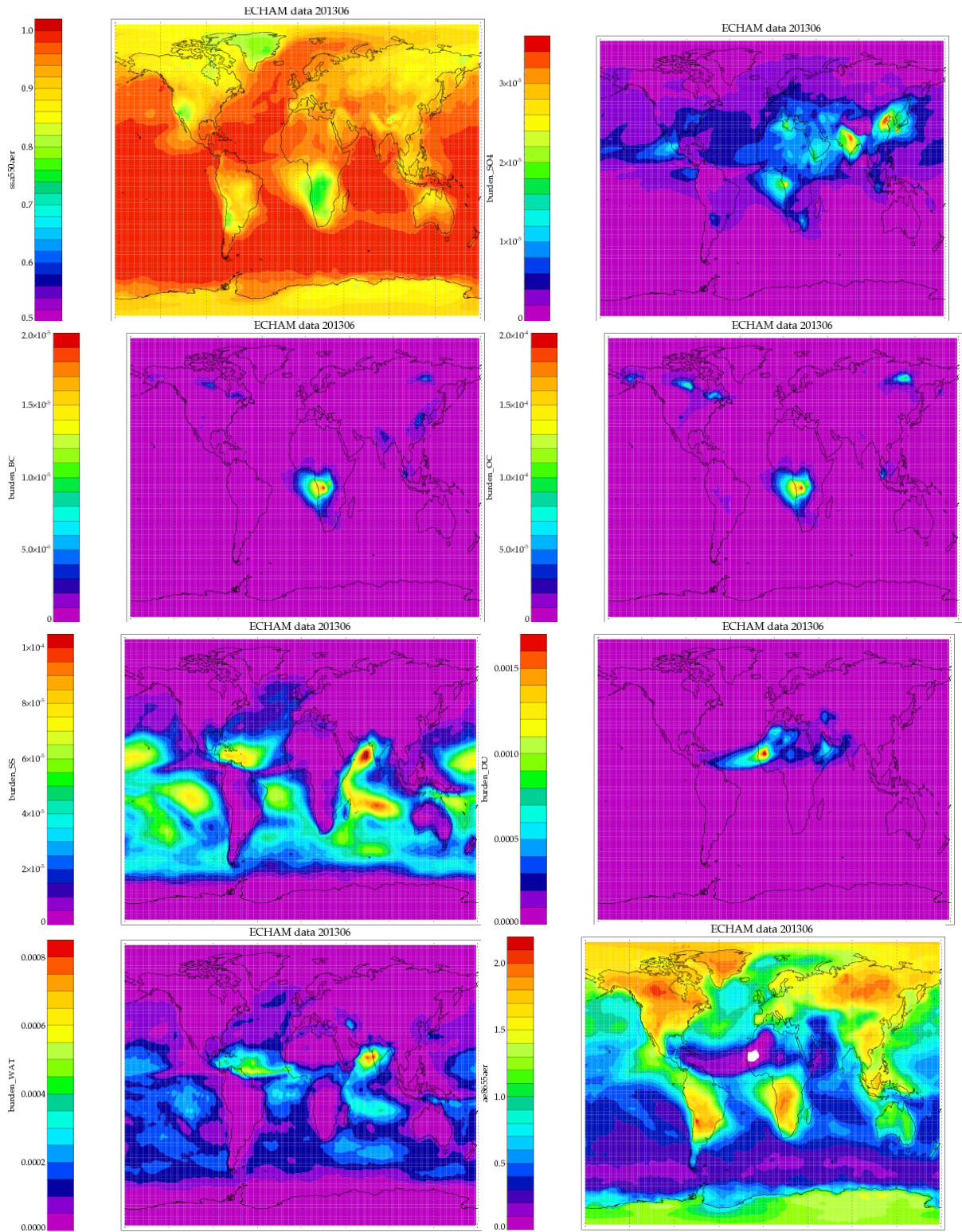


Figure 8 ECHAM Model fields for June 2013 row1: Single scattering albedo and  $SO_4$  burden, row2: BC burden and OC burden, row3: SS burden and DU burden, row4: WAT burden and Angstrom exponent.

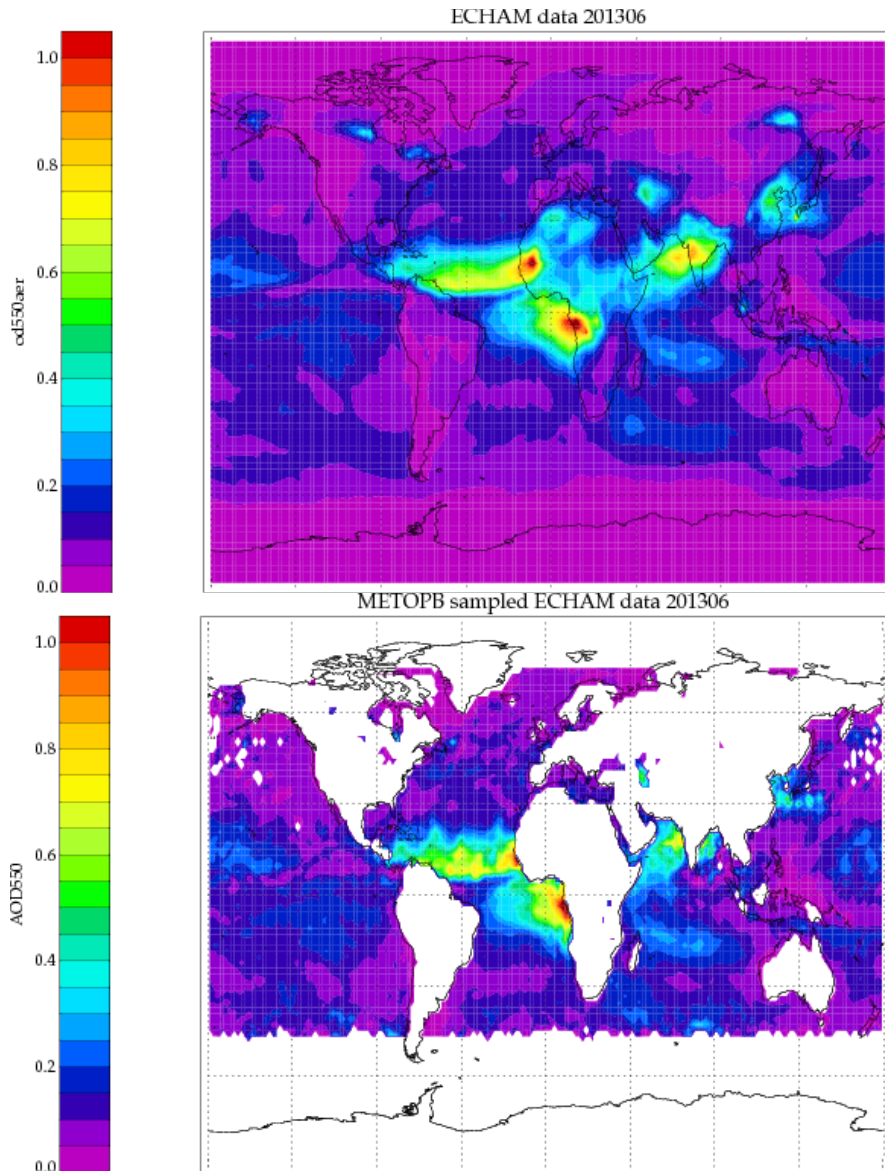


Figure 9 ECHAM Aerosol Optical depth averaged for June 2013 (top) and ECHAM model data sampled with METOP swath .

### 3.3. RESULTS OF JUNE/JULY 2013 METOP-A AND METOP-B COMPARISON

Figure 10 and Figure 11 show global results for June and July 2013. On the left hand side are comparisons for Metop-A and on the right Metop-B. The plots indicates that globally, the Metop-A aerosol observations compare more favourably than Metop-B with model results, with Metop-B results positively offset compared to the model. We note that the difference in the satellite AOD is often larger than in the model/satellite difference AOD.

The differences between Metop-A and Metop-B are caused by differences in calibration for the two instruments.[Ref-14]. Aerosol retrievals are very sensitive to the calibration of the satellite instrument. The results would suggest that there is a positive bias in the calibration of the Metop-B instrument. In the interests of clarity the results from this point on will be shown for the Metop-A instruments however the results have generated and are available for all satellites.

A number of initial observations are apparent from the global maps

1. For the time series globally the satellite and model results show excellent general agreement however this global view masks a number of compensating effects which are hinted at in the scatter plot. i.e at very small aerosol optical depths the satellite data is positively biased compared to model while at high AOD values the reverse is true.
2. The model predicts higher AOD in the Saharan dust outflow region
3. The model predicts higher AOD in the Central African biomass burning region
4. The model AOD is positively offset compared to satellite observations over sea in the southern hemisphere where the air is relative 'clean' the sea salt overestimation is likely a model emission issue while in the more polluted Northern hemisphere the model AOD shows a negative difference which is likely an under estimation of air pollution more likely a model deficiency.
5. Coastal outflow regions located in China and Indonesia show higher satellite AOD than model AOD. From earlier plots, the model does quite well with respect to the Saharan dust outflows and Central African biomass burning region. On the other hand, it is known that the model overestimates AOD over most of the oceans. For reason alluded to above (e.g. lack of nitrates in the model, the model also underestimates AOD over pollution regions like China, the underestimation of pollution is more likely a model deficiency.
6. The model predicts a region of high AOD outflow off the coast of east Africa that extends over the Indian ocean towards Madagascar and Australia. This 'plume' is not visible in the satellite data. Fig.8, especially the water burden, suggests that this plume is due to elevated relative humidity and the associated wet growth of sea salt aerosol (the most wettable aerosol in the model)

From the collocated model data we can see the most dominant aerosol type is water (WAT) followed by sea salt (SS). In the model, water is not considered an aerosol species in its own right: most aerosol models including ECHAM, do not prognostically carry aerosol water but estimate it from current conditions: relative humidity and the hygroscopic properties of the 'real' aerosol species (SS,DU,OC,BC,SO<sub>4</sub>). Aerosol water will still have a big impact of AOD. It should be noted that the relationship between the mass of different aerosol types is not linearly related to aerosol optical depth rather the relationship is non linear and depends on various factors such as particle size and refractive index. Aerosol optical properties are calculated each time-step based on the mixing state of the species in the various modes and the typical size of these modes. Both mixing states and size are calculated by the model as a result of the various aerosol processes. What is assumed are the refractive indices of the various species (A volume-mixing approach is used to determine the refractive index of mixed species) and the spread of the log-normal mode (which is constant). Again based on the mixing state of a mode, its ability to attract water and grow with relative humidity is calculated based on the relevant species.

Figure 12 shows the difference between Model collocated Metop-B and Metop-A ( and satellite Metop-B and Metop-A for June 2013. These plots give an indication of how variable the aerosol is between orbits. The difference is mostly very small except in regions with typically high aerosol loadings such as dust and biomass burning. The Metop-A and Metop-B difference plot show a systematic positive offset globally.

Figure 13 shows the standard deviation of aerosol optical depth for a single month, June 2013, of collocated model data and Metop-A data. The model data unsurprisingly shows much less variance with the high values of variance occurring in regions of dust and pollution outflow. The satellite variance shows similar patterns although higher variance overall. The high values occur in the southern hemisphere storm tracks, southern tropics and tropics in regions of measured small aerosol loadings would indicate the presence of cloud contaminated measurements, or greater temporal variation of aerosol.

A more detailed discussion of the differences is undertaken with reference to the regional statistics outlined further in this section. The regions have been carefully selected to examine the agreement or lack of as a function of aerosol regime. Note caution must be taken in interpreting the results for the regions as the region area decreases as the number of observations used to calculate the daily average can be small.

Figure 14 shows the difference between 2010 and 2013 retrievals for the same month, the differences are quite striking, in 2010 the Saharan dust outflow was significant larger than in 2013. While in 2013 the North Atlantic has significantly higher aerosol loadings that were caused by unusually extensive Canadian wildfires, the smoke from these wild fires was detected in Europe (<http://www.sciencedaily.com/releases/2013/07/130712084344.htm>). Both the model and the satellite data observe these events although the magnitude and spatial distribution differs slightly. More dust in the model and larger spread of the wildfire smoke in the satellite data.

Common to both years to the west of the North American coast are high aerosol loading in the satellite data and low values in the model data. The number of satellite observations in this region is low because of the predominance low warm clouds in this region that are difficult to identify and clear.

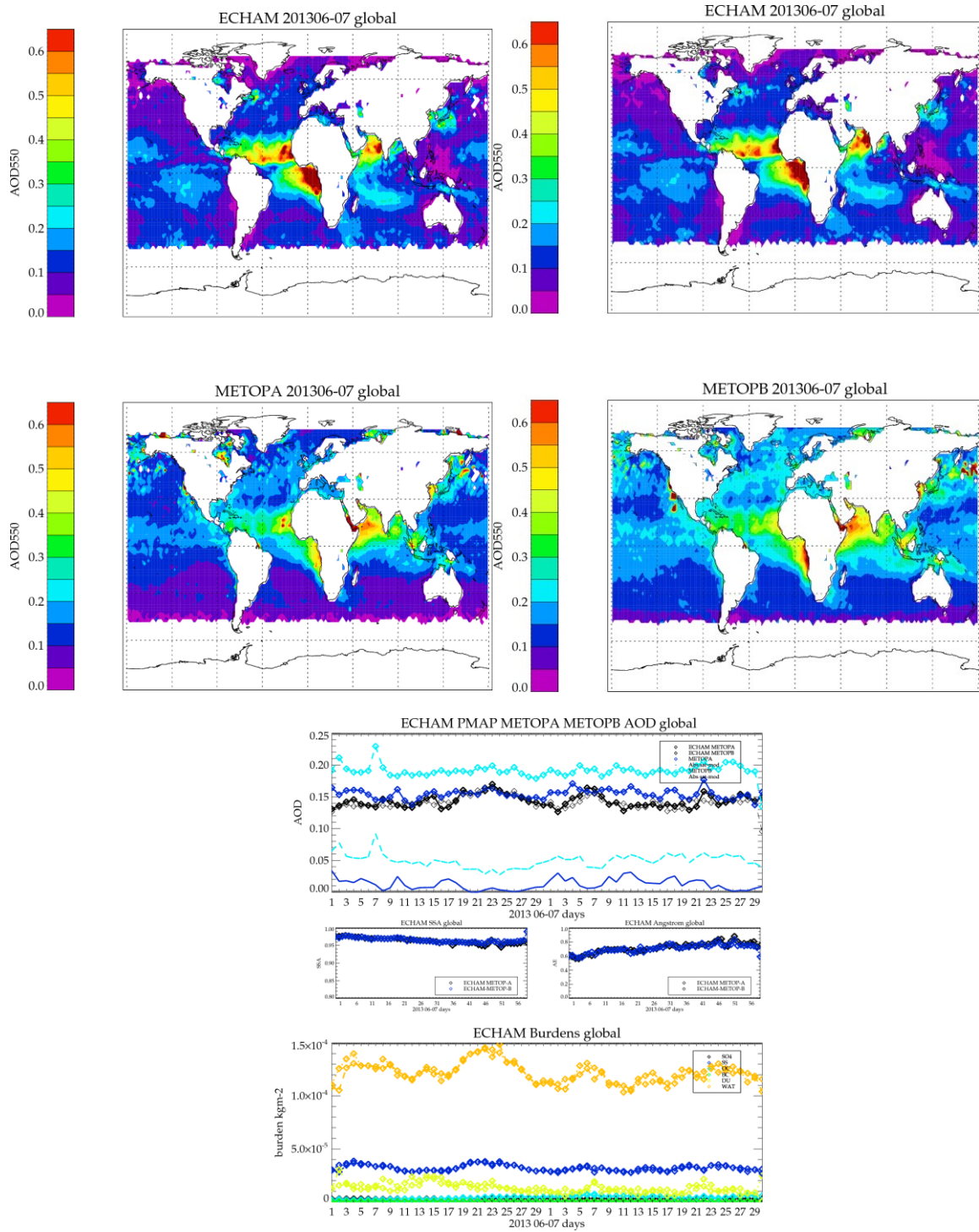


Figure 10 Comparison of Metop-A left, and Metop-B right, aerosol optical depth and ECHAM model for June 2013. The AOD time series shows in black Metop-A Model collocations, in grey Metop-B model collocations, Dark blue shows the Metop A satellite results and associated difference with the model. Pale Blue show the Metop-B satellite results and associated model difference. The next 2 plots

show the SSA and AE of the model collocated with Metop-A black and Metop-B blue. The burdens plot shows the model speciation for Metop-A collocations (solid line) and Metop-B collocations (dashed line).

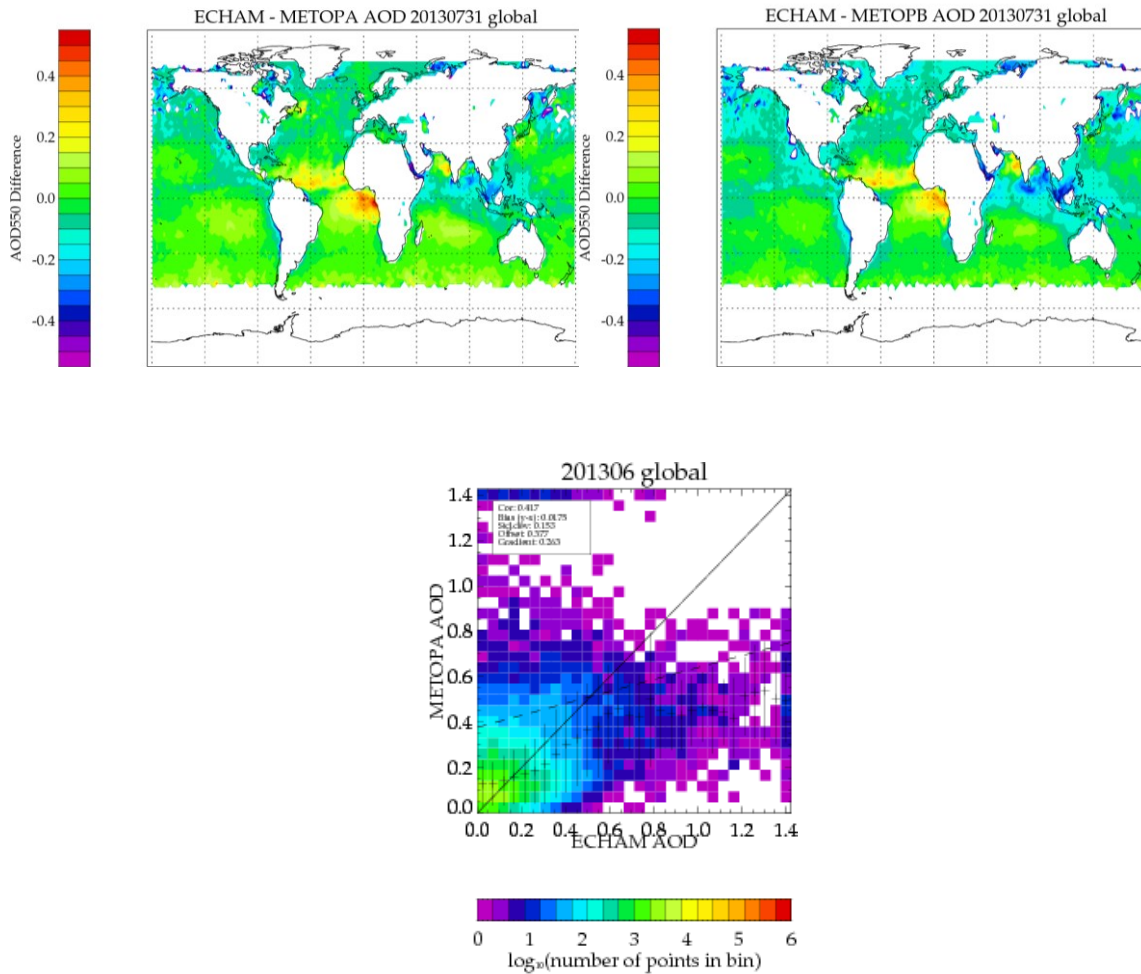


Figure 11 Difference between Metop-A (top left) and Metop-B (top right) satellite and ECHAM data. On the bottom row a scatter plot derived from level 2 swaths for the whole month.

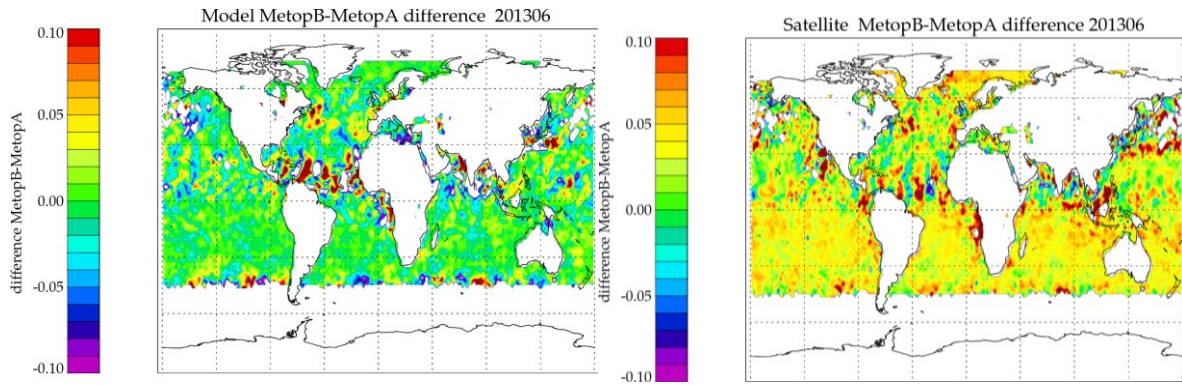


Figure 12 Difference between Model collocated Metop-B and Metop-A (left) and satellite Metop-B and Metop-A (right) for June 2013.

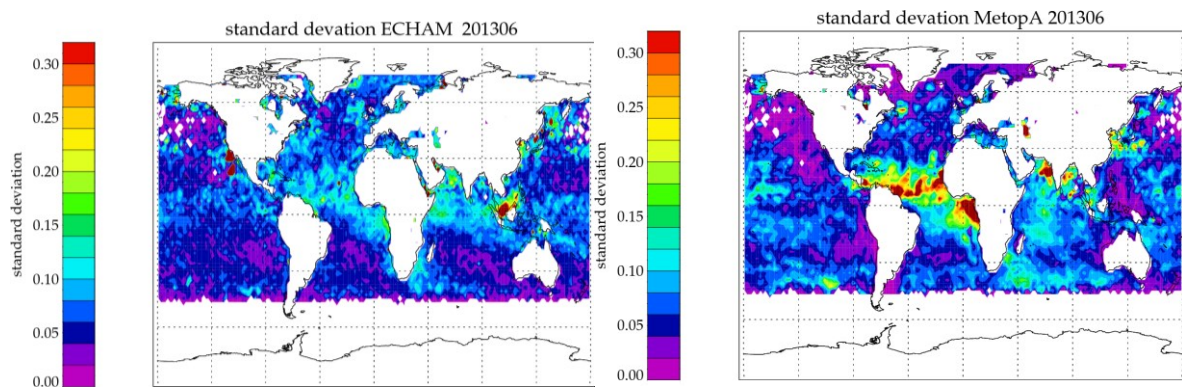


Figure 13 Standard deviation of one month, June 2013 collocated model data (left) and Metop-A data (right).

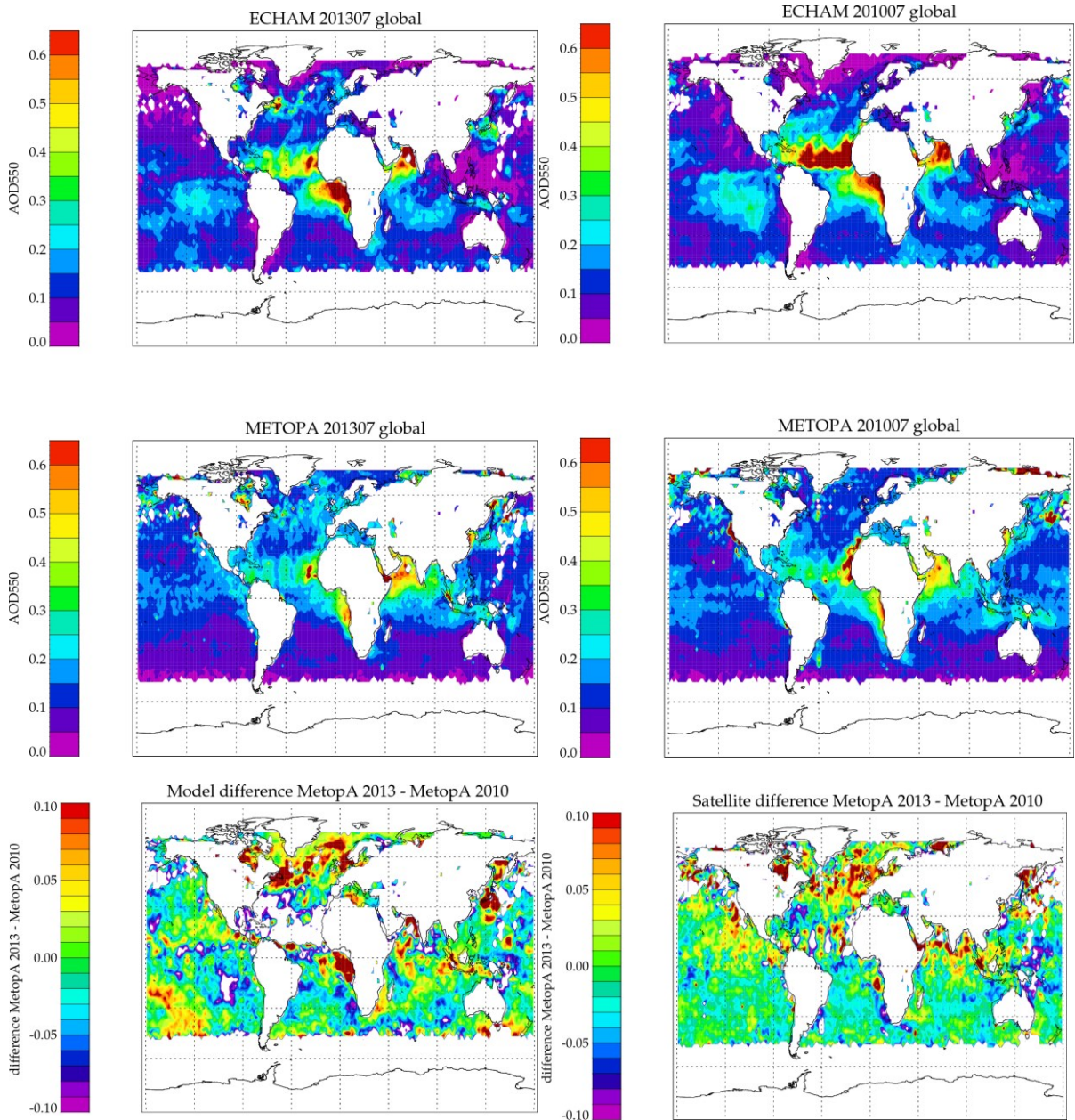
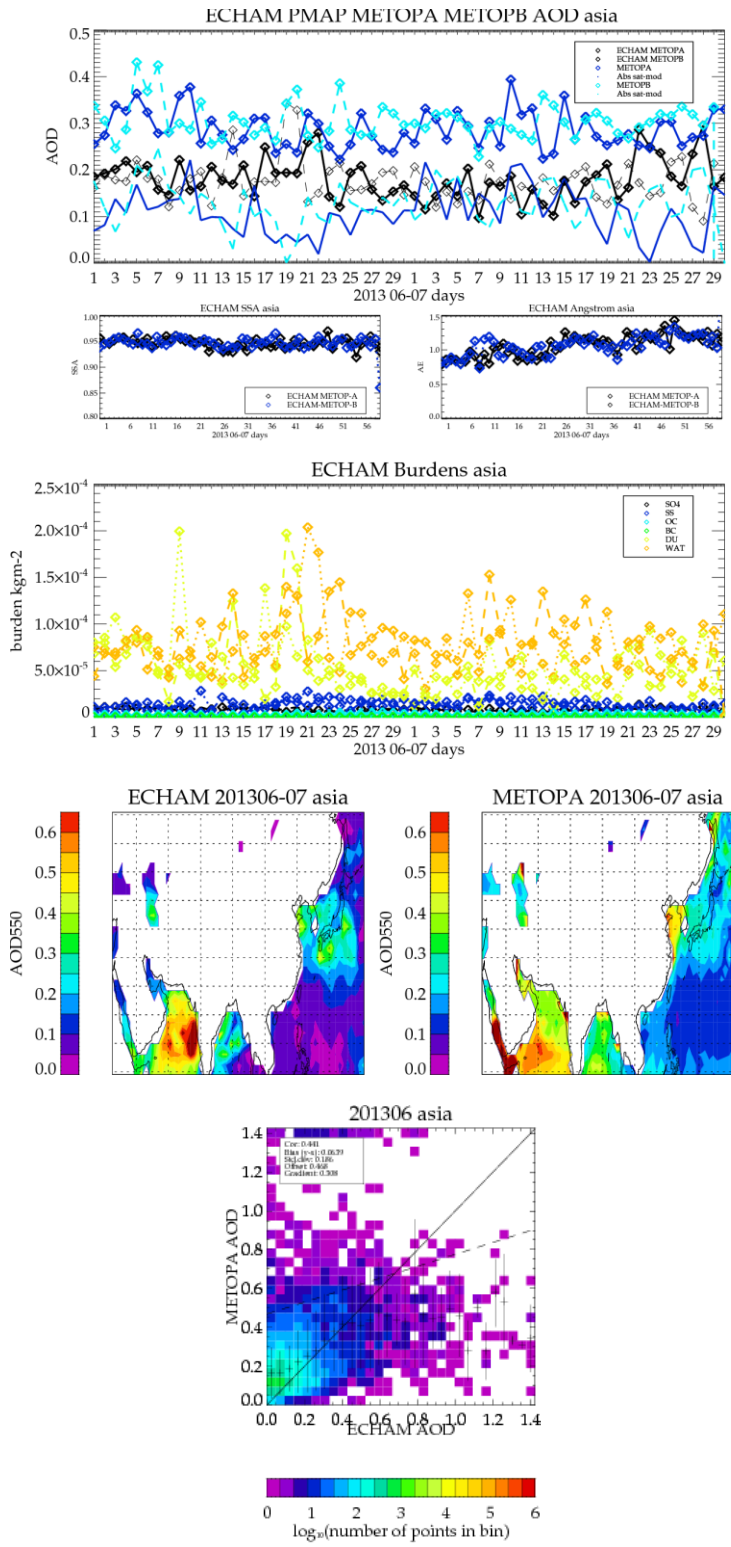


Figure 14 Comparison of Model and Metop-A satellite data for July 2013 with July 2010. Model data (top row) Satellite data (middle row) Model 2013-2010 (bottom left), Satellite 2013-2010 (bottom right)

### 3.4. REGIONAL ANALYSIS



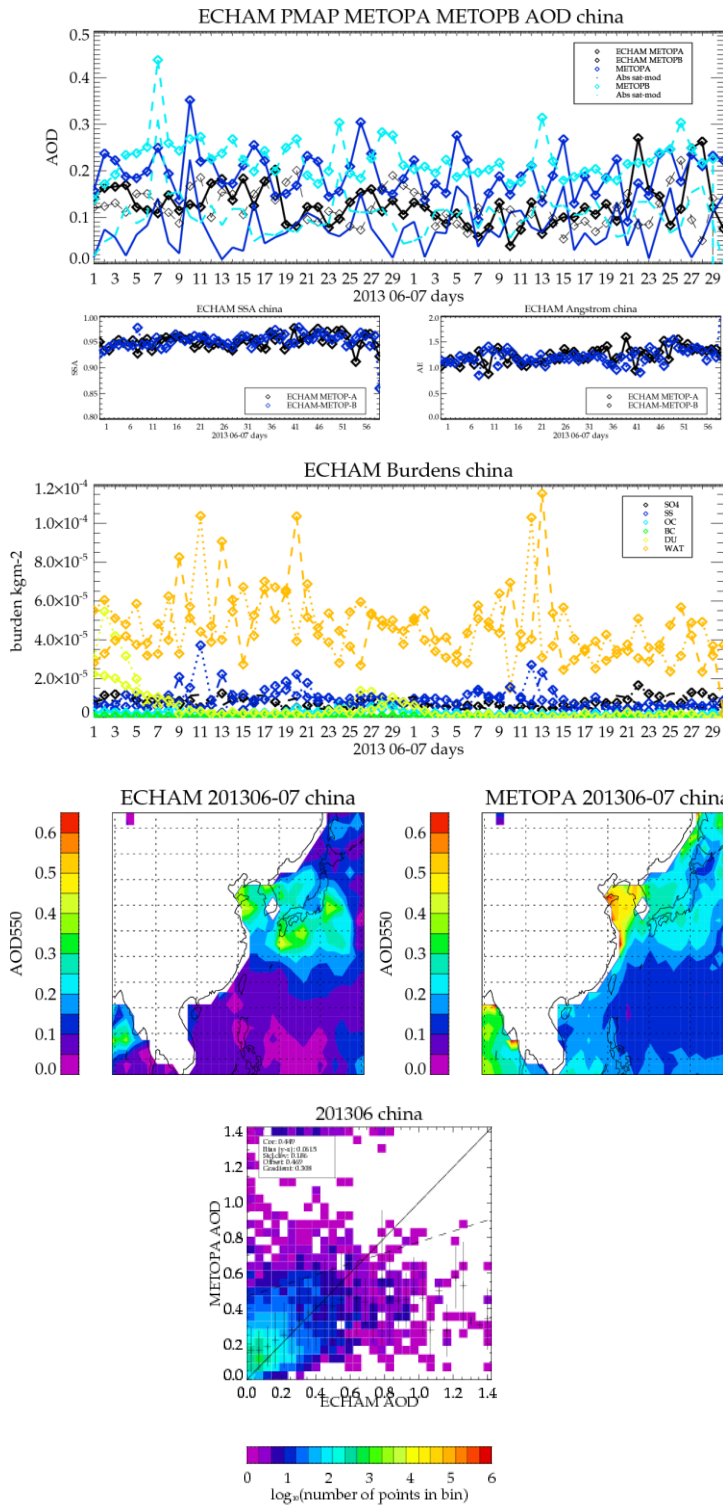
Figures to the left show a regional comparison over the **Asian** region. After water, dust (DU) is the dominant aerosol type, there are slightly elevated levels of the other aerosol types, sulphate (SO4), organic carbon (OC) and black carbon(BC).

The satellite observations are typically .05 to .1 higher than the model results. With the background value over sea generally higher as well as, close to the coast.

The model is known to underestimate aerosol in polluted regions so this bias is expected.

The satellite data features two hotspots in the satellite data (not visible in the model data), north of Japan, east of the kurils. This is mainly open ocean, although quite some oil drilling is going on in that region which might produce high values.

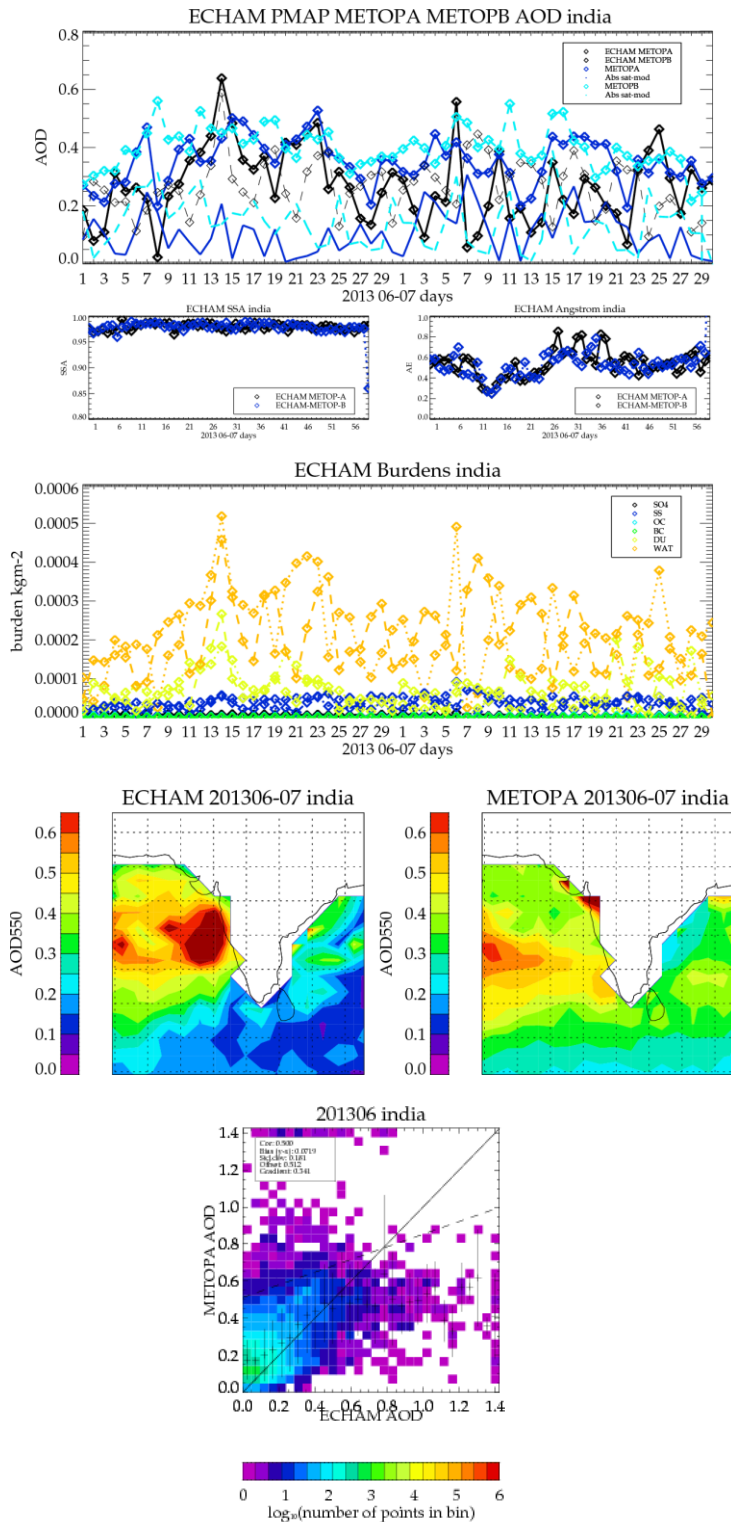
**Figure 15 Metop-A Asia results.** The top plot shows the AOD time series, Black Metop-A Model, grey Metop-B model, Dark blue shows the Metop A satellite results and associated difference with the model. Pale Blue show the Metop-B satellite results and associated model difference. The next 2 plots show the SSA and AE of the model collocated with Metop-A black and Metop-B blue. The burdens plot shows the model speciation for Metop-A collocations (solid line) and Metop-B collocations (dashed line). The maps show the regions distribution of AOD for the model (left) and satellite (right) and the scatter plot shows the correlation as a function of model grid point.



This figure focusses in on the **Chinese coast** where sulphate type aerosols are a significant factor. The satellite observations show elevated aerosol amounts compared with the model,

The model is known to underestimate aerosol in polluted regions so this bias is expected. ECHAM-HAM uses a simplified treatment of VOCs and in addition does not include nitrate as aerosol. Both issues are likely to cause underestimation of AOD. See also the model evaluation against MODIS and AERONET.

Figure 16 Metop-A China results. The description of the plots is the same as for Figure 15.

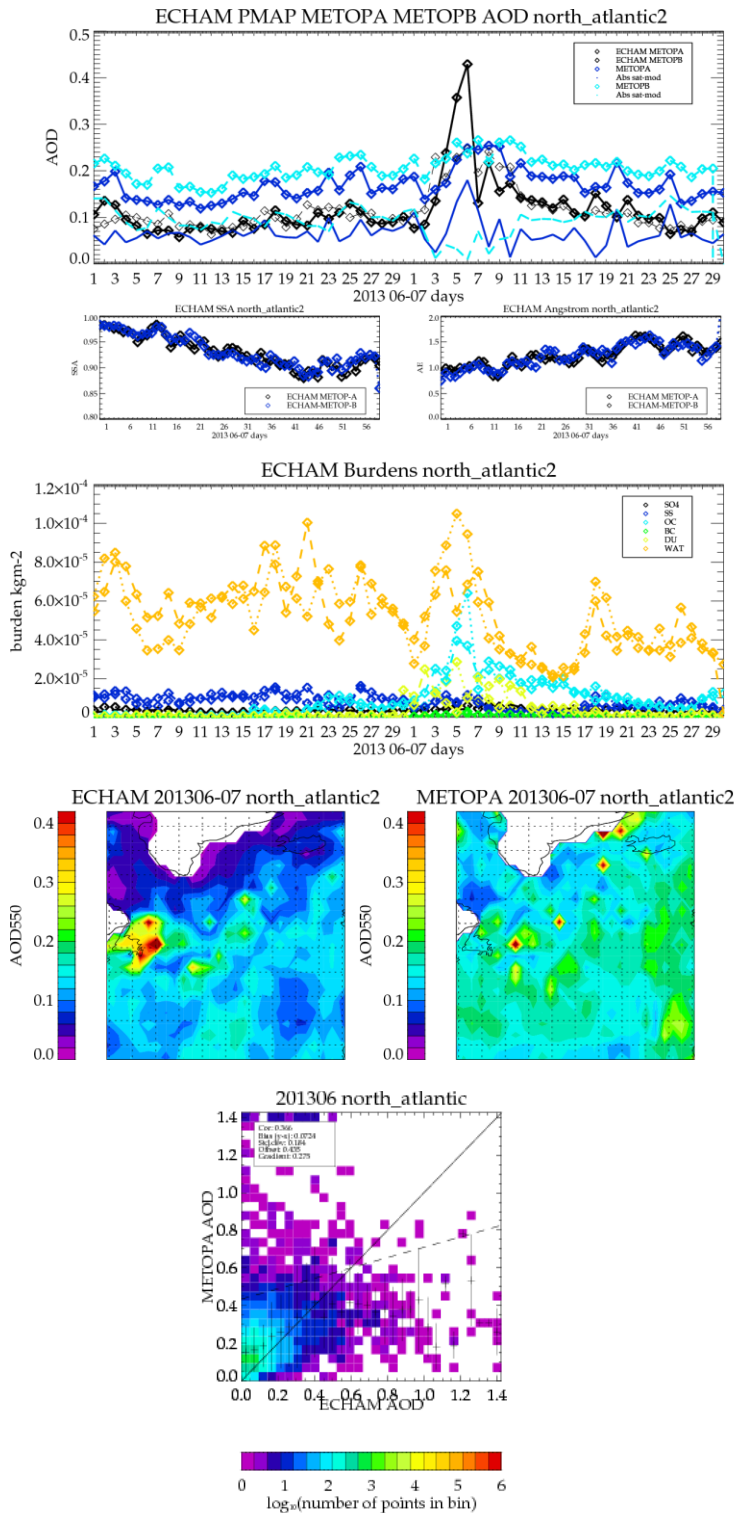


This region centred on **India** shows reasonable agreement between satellite and model however the spatial patterns are quite different, giving rise to a number of compensating effects reflected in the calculation of the daily average.

India is a difficult region to model AOD because of the unique local meteorology and the local dynamics which are heavily influenced by the Himalayas Significant contributions of aerosol originate from neighbouring Africa. AOD monitoring is important for this region because of the large population and air quality issues so there is considerable interest in evaluating and using satellite AOD retrievals in this region.

Metop detects some high aerosol close to the coast in the region of India where high AOD would be expected however the highest aerosol loadings appear to originate from Africa. This could be a case where the cloud mask is over conservative and removing high anthropogenic and biomass aerosol.

Figure 17 Metop-A India results. The description of the plots is the same as for Figure 15.



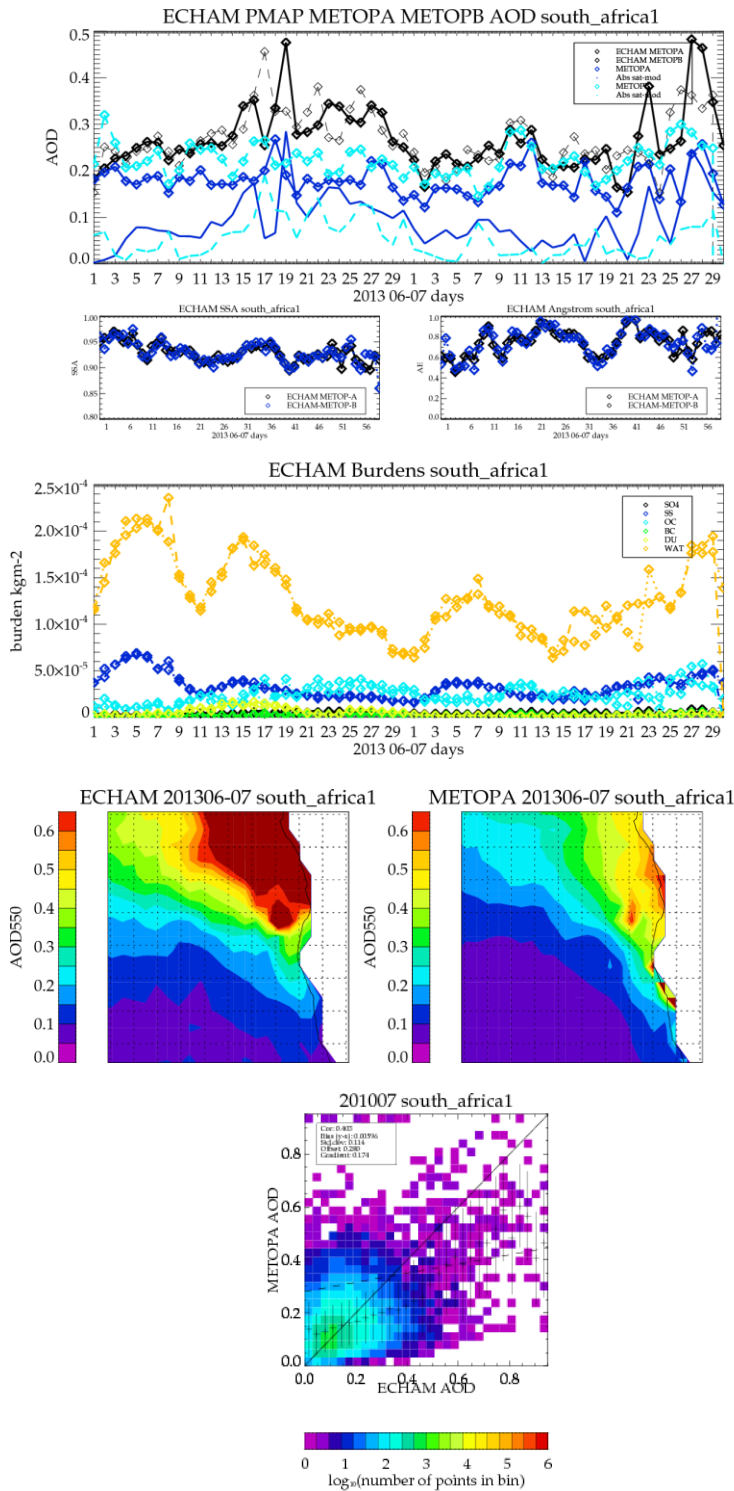
The **North Atlantic** region shows distinctive changes over time in June the satellite data is offset compared to the model which likely under estimates polluted ocean atmosphere.

In July the aerosol loading increases with significant contribution according to the model from organic carbon. This corresponds to the occurrence of extensive wildfires in Canada creating smoke that was eventually detected in Europe. The aerosol become more absorbing over these 2 months and the particles smaller.

Except at the beginning of July the model has consistently smaller AOD than the satellite data.

Correctly modelling wildfires in boreal America has proven to be challenging. This is likely due to the large uncertainty in the emission inventories which in turn is due to problematic observation of smaller and low intensity fires (compared to e.g. the fires in the Amazon).

Figure 18 Metop-A North Atlantic results. The description of the plots is the same as for Figure 15.



These figures are for the **African biomass region south of the equator**. Originally the Southern African biomass region was considered as a single zone. However further analysis has shown that the regions south and north of the equator are quite distinct.

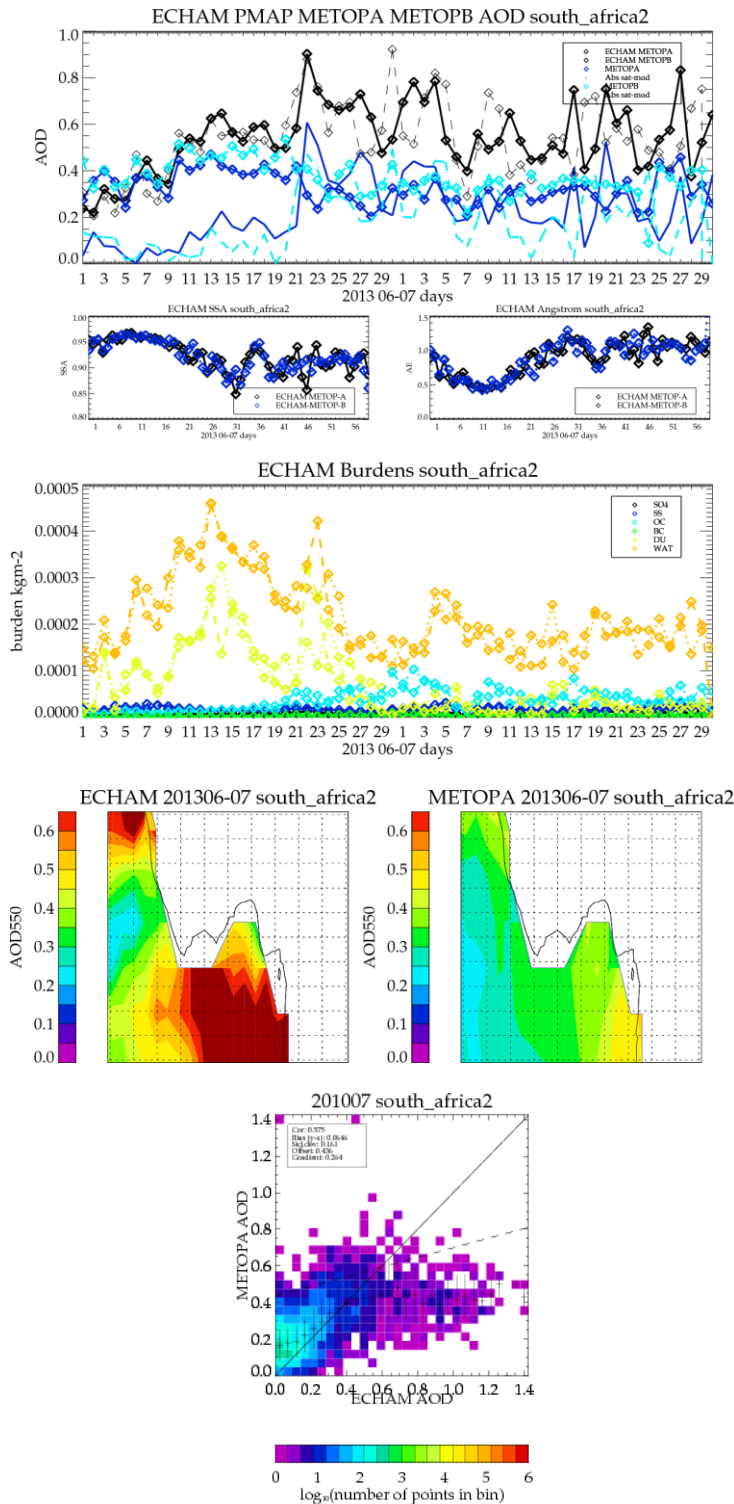
The model AOD for this biomass region has a similar spatial pattern, although the satellite data extends further south. On average the model aerosol values are positively offset to the satellite AOD.

The aerosol types in this region are quite mixed with significant contributions from both sea salt and significantly organic carbon which increases the absorption (decreases the SSA).

Uncertainty in satellite retrievals can be caused by theselection of correct optical properties used in the retrieval. If the aerosol type used in the satellite retrieval is not sufficiently absorbing the satellite AOD will be underestimated (over a dark surface)

There is also considerable uncertainty in the model values over water (ie. outflow). The model overestimates AOD compared to MODIS but over land (see also time-series in section on ECHAM) it does quite well. It maybe that this is due to an overestimation of SS.

Figure 19 Metop-A Southern African biomass region south of the equator. The description of the plots is the same as for Figure 15.



These figures are for the **biomass region North of the equator.**

This region, the Sahel, is extremely complicated with contributions from both dust (scattering) and carbon (absorbing aerosols)

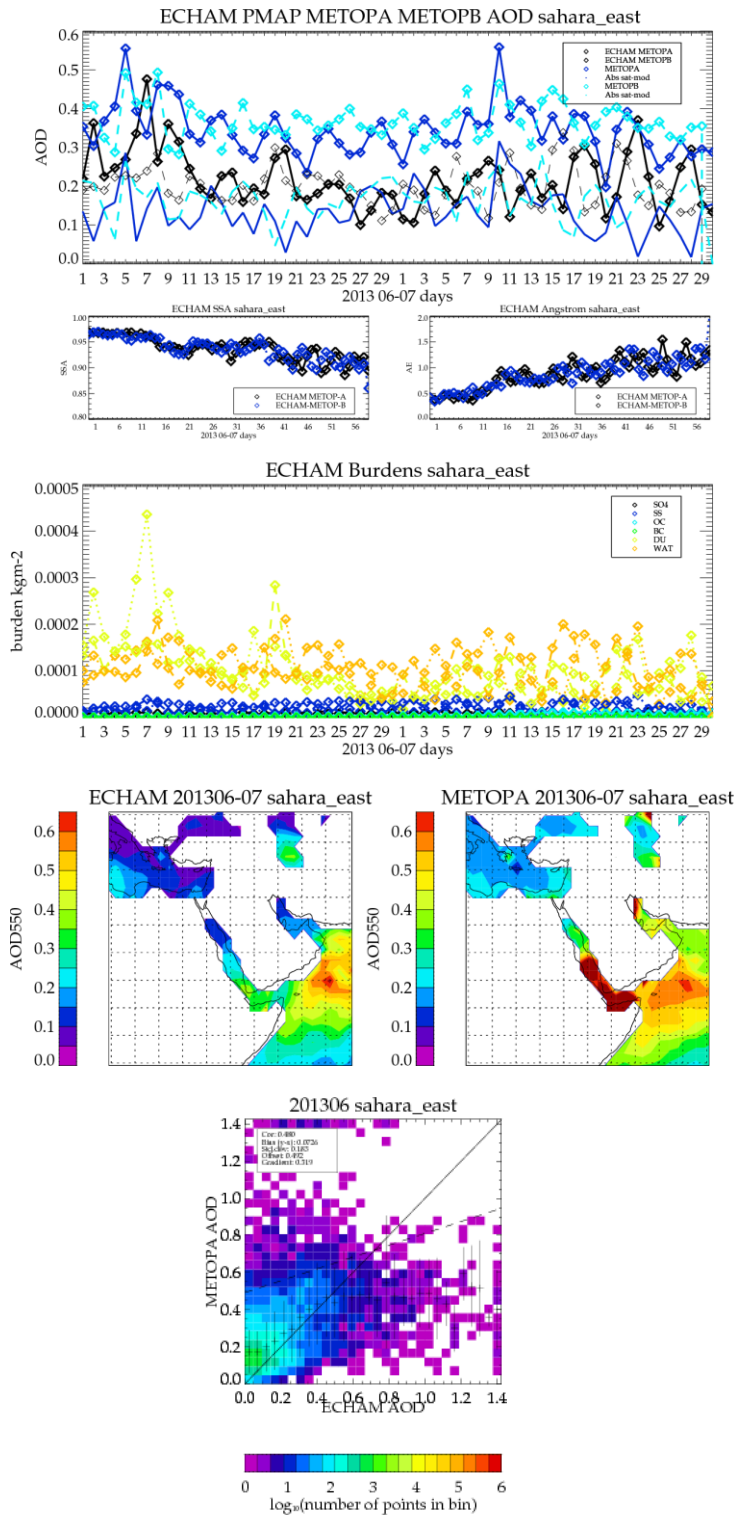
The AOD values in the model and satellite are generally higher in this region. There is good agreement at the start of the month however the values begin to diverge strongly when first a significant contribution from dust and then increased organic carbon are predicted in the model.

Cloud screening and selecting the correct optical properties for an accurate satellite retrieval will be challenging for this region: the selection of aerosol type could be critical for this region.

There is also model uncertainty. If we assumed the satellite values to be correct this would suggest too much contribution from organic carbon in the model.

In the model validation over water (ie. outflow) the model overestimates AOD compared to MODIS. It may be that this is again due to an overestimation of SS, which appears to be a global issue, coupled with an overestimation of wet growth due to humidity

**Figure 20 Metop-A Southern African biomass region south of the equator. The description of the plots is the same as for Figure 15.**



In the **Eastern Saharan outflow** region the model is indicating that dust is the dominant aerosol type. The particles start off large at the start of the month and decrease in size together with AOD until the end of the month.

The satellite observations of the dust have a higher optical depth than the model observations. This could indicate that the emission data bases or dust source maps for this region underestimate the aerosol optical depth in the model (Previous Aeronet- Model comparison suggests that ECHAM-HAM does fairly well in the west part of the Sahara, at least when averaging over a week and a large region: ECHAM-HAM also agrees nicely with MODIS and AERONET AOD peaks. In the east part, tending to underestimate AOD (esp. its summer peak), although the model follows the yearly cycle reasonably well. Dust modelling is inherently difficult and it is possible that small dust events can be predicted entirely incorrectly. No inventories are used for dust emissions, instead parameterisations based on wind speed, soil moisture are used to model dust in the models. In addition a dust source map is used to indicate where emission can potentially happen. [REF-13]. As the values in this region are lower in general than the Western Sahara, cloud flagging is less likely to be an issue.

Figure 21 Metop-A Eastern Sahara region. The description of the plots is the same as for Figure 15.

The Saharan dust region is divided into two zones one close to the coast and the second some distance from the coast to evaluate the particle deposition in the model.

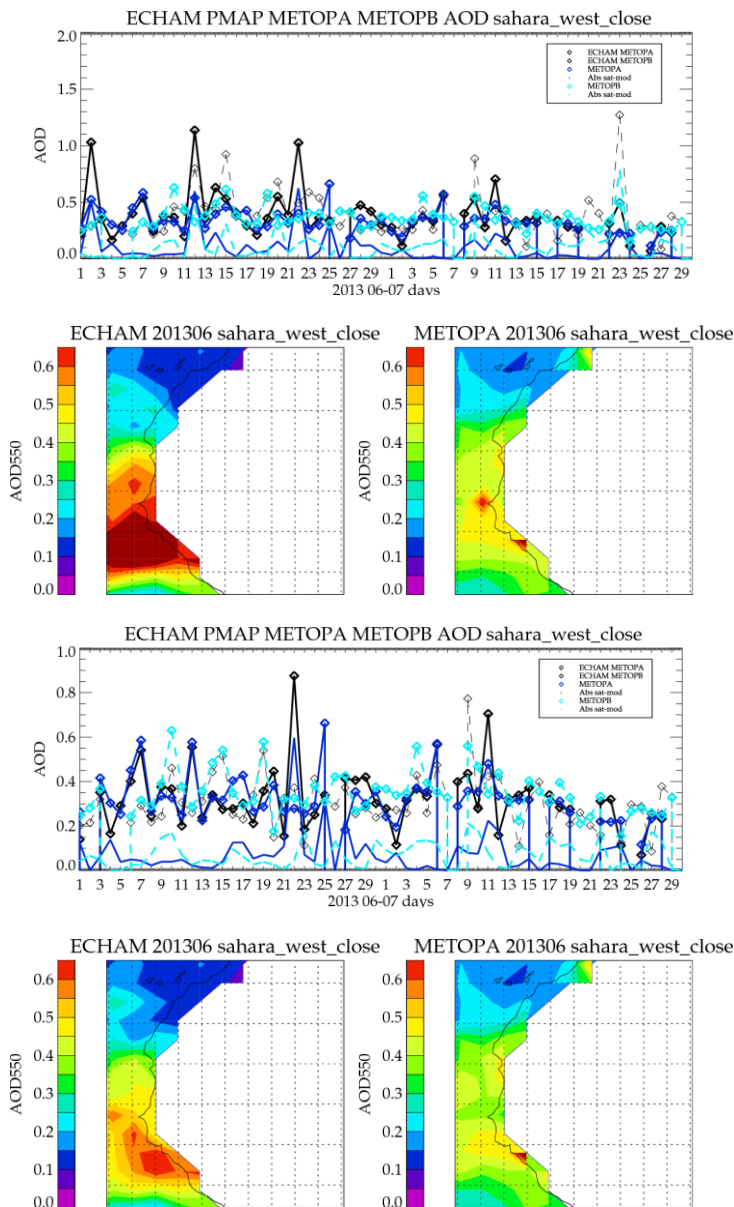


Figure 22 Metop-A Western Sahara outflow close to the coast, June/July 2013 results. The top plots show the straightforward comparison with the model the bottom 2 plots show the comparison when collocations with a model AOD > 1.0 are removed. Note the different y-axis ranges in the time series plots

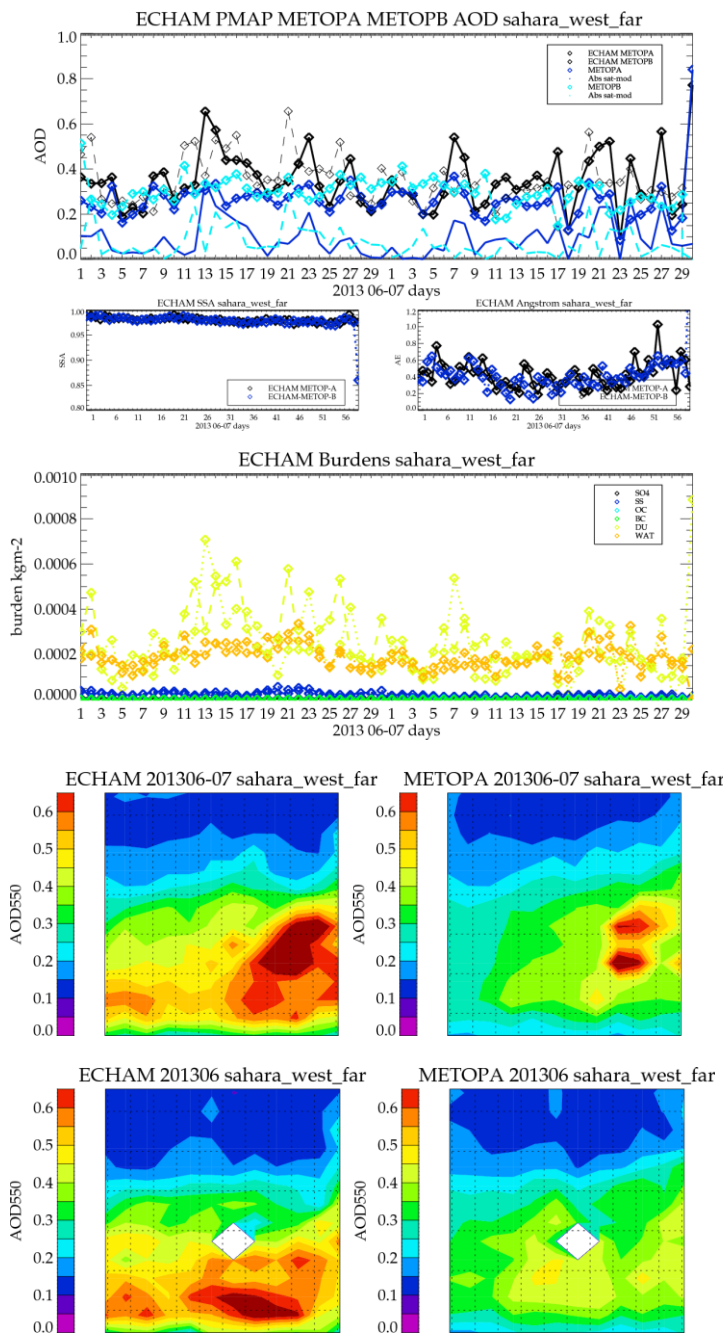
Close to the **West Saharan** coast the satellite observations agree well with the model except when the model predicts very high aerosol events.

There are 2 possible scenarios

1) The satellite observations in this region have been conservatively cloud screened thus removing some high aerosol optical depths. This scenario would not be picked up by standard Aeronet comparisons that rely on both sets of data to be cloud free.

2) The model is creating spurious high aerosol events. While the AERONET sites in front of the coast show that the model has a high correlation with Aeronet however in the Summer months there are indications that the model is too high.

The bottom 2 plots show the comparison for model collocations when model AOD > 1.0 are removed. The correlation with satellite observations is much improved. MSG 'pink' imagery was inspected for the days with model AOD > 1. These days did not exhibit anomalously high dust plumes, hence we conclude that the model AOD is too high. This is consistent with the model/Aeronet comparison for this region shown in [Figure 5](#)



This **Saharan dust** further from the source shows similar results to the region closer to the coast however the spikes are not as significant and the aerosol loadings smaller as would be expected as the aerosol is deposited in the ocean. It is encouraging that the size of the particles predicted in the model also decreases further from the coast.

As the aerosol optical depth decreases so the effect of removing aerosol optical depths greater than 1.0 in the model does not have as big an impact. The ECHAM AOD is still significantly higher than the satellite results however this is likely caused by the model transporting the remnant of the originally much larger plume in the model.

Figure 27 shows the global maps with model AOD > 1.0 removed. Interestingly the satellite AOD values change very little globally while the model AOD decreases significantly in dust and biomass regions.

Figure 23 Metop-A Western Sahara outflow far from the coast, June 2013 results. The top plot shows the time series of satellite and model collocations while the bottom 2 plots show the regional distribution of AOD first for the complete set of collocation and at the very bottom with Model AOD values > 1.0 removed.

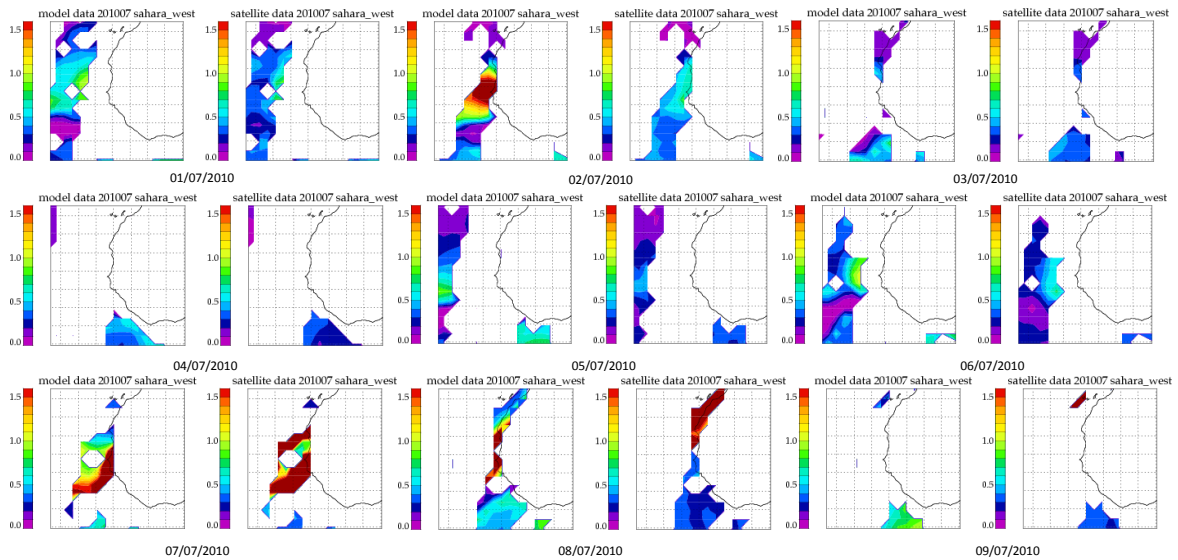


**Figure 24** Daily collocations of ECHAM model data and Metop-A retrievals. Top row, 1<sup>st</sup>-3<sup>rd</sup> July 2010, Middle row 4<sup>th</sup>-6<sup>th</sup> July 2010, Bottom row 7<sup>th</sup>-9<sup>th</sup> July 2010.

In order to investigate the difference in detecting Saharan dust plumes a large Saharan dust storm identified in June 2010 was analysed in further detail. Figure 24 shows daily collocations between the 1<sup>st</sup> and 9<sup>th</sup> of July for a large dust squall, a spectacular animation of the dust squall from SEVIRI can be observed over the ocean from the 6<sup>th</sup> to 9<sup>th</sup> of July 2010 at this web address

[http://www.eumetsat.int/website/home/Images/ImageLibrary/DAT\\_IL\\_10\\_07\\_05.html](http://www.eumetsat.int/website/home/Images/ImageLibrary/DAT_IL_10_07_05.html). The pattern of the dust is captured well by Metop-A. The largest satellite AOD loadings are observed on the 7<sup>th</sup> and 8<sup>th</sup> in the correct locations. The elevated AOD values observed on the 2<sup>nd</sup> of July are not apparent in the Metop-A of SEVIRI imagery, suggesting the superiority of the satellite data in this case. Note that the collocations are only possible where there is no cloud. This would be a good case to evaluate when land retrievals become available.

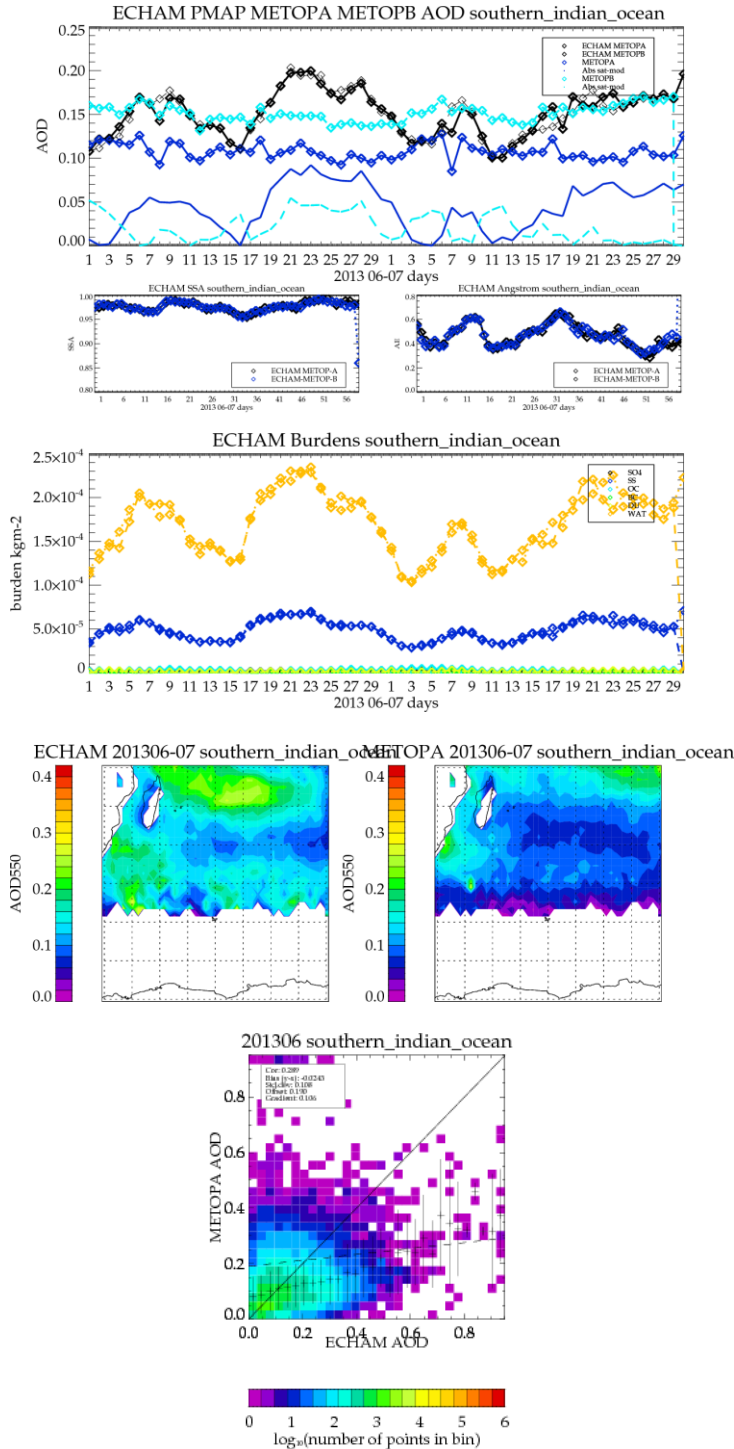


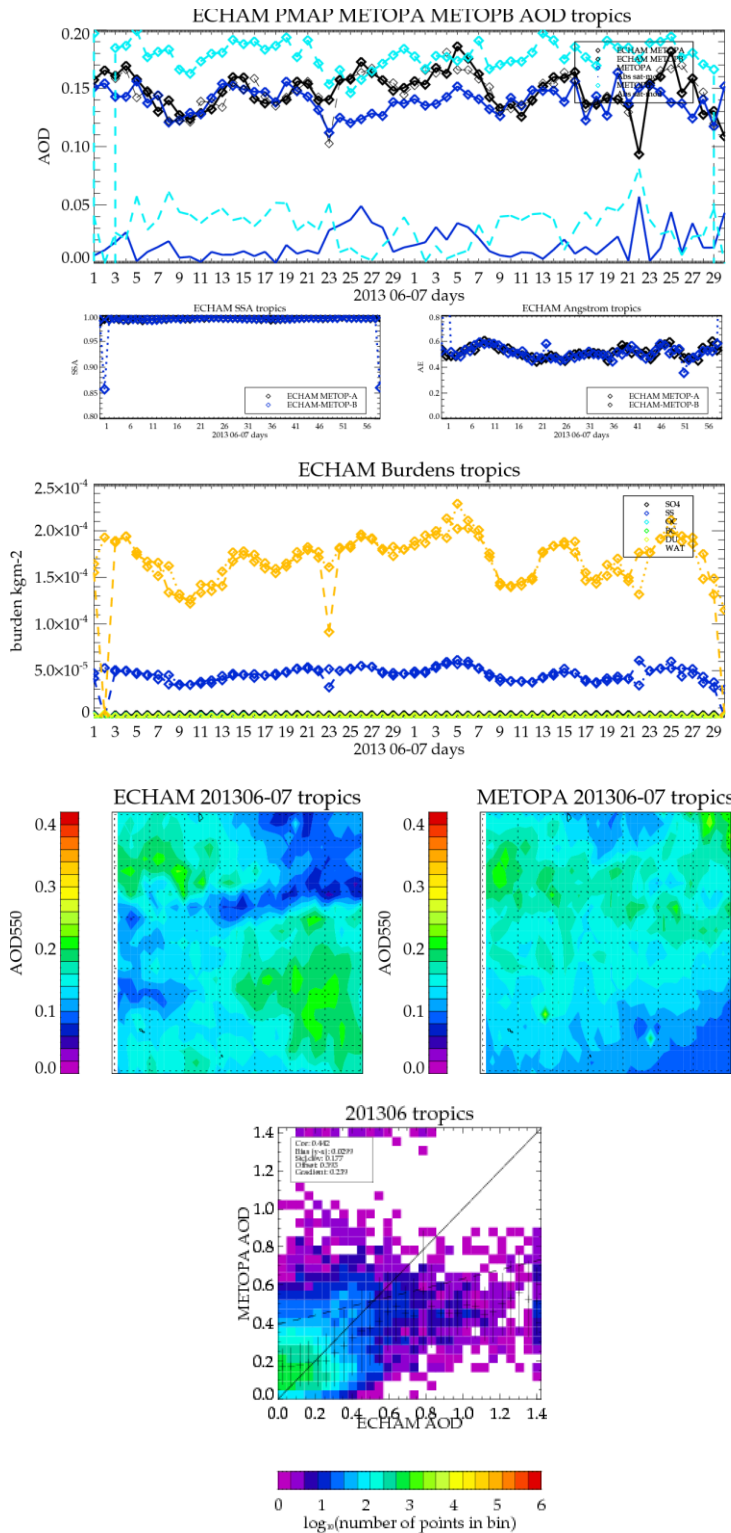
**Figure 25 Southern Indian ocean region, June 2013.**  
 The description of the plots is the same as for Figure 15.

Globally over the **Southern clean open oceans** the model AOD is higher than the satellite AOD.

The satellite data is fairly constant while the model data varies with the variance significantly correlated with the burdens of water and sea salt. We would expect that the AOD over remote oceans is dependent on local meteorology, both wind speeds and humidity. Sea salt is one of the most hygroscopic aerosols, more-over it also exhibits hysteresis as relative humidity changes (this is not modelled in ECHAM\_HAM) i.e. increases and decreases in relative humidity lead to different wet growth of the aerosol. Furthermore, the large 200 by 200km grid boxes do not allow wind speed variations over 10km to impact sea salt emissions. We would expect the satellite observations to mimic this variance in AOD with relative humidity however this is not seen.

This southerly ocean regions are typically dominated by the southern hemisphere storm tracks and associated high cloud amounts which traditionally make satellite cloud clearing quite difficult. This is not observed in this region of the remote ocean suggesting the model is too high.

The strong cyclical nature of aerosol water in the model, is mostly the result of an identical cycle in seasalt (i.e. relative humidity changes are rather unimportant), which itself is mainly due to prevailing windspeeds. In-depth evaluation of this aspect of the model is suggested as a future study.



This analysis covers a large **tropical ocean** region to the east of central America. 20 degrees  $\pm$  north and south of the equator -180 to -110 degrees East

This region is relatively Open Ocean however it can have a small contribution of far easterly blown Saharan dust.

The model and satellite data agree very well on average in this region however the scatter plot indicates that some positive and negative biases are cancelling out.

This region may have cirrus contamination in the satellite data causing a positive bias, suggestions of this are visible in the AOD standard deviation plots (Figure 13) while the model data may have problems with SS

Figure 26 Metop-A tropical ocean results. The description of the plots is the same as for Figure 15.

### 3.5. RESULTS OF JUNE 2010 METOP-A AND AATSR COMPARISON

In addition to model comparisons it is useful to compare the PMAp data set to other existing Aerosol data sets to confirm and support hypothesis. The AATSR ORAC CCI aerosol product is well placed for such a comparison for while a number of similarities exist between the products, for example they both utilise the visible to near infrared spectral region and as such have a similar information content however a number of differences exist, the AATSR algorithm has a 10kmx10km resolution and the algorithm utilises the dual view to obtain accurate atmospheric correction. To obtain the best spatial coverage the comparison was performed indirectly i.e both satellites were collocated with ECHAM separately and the comparison performed at model resolution. Figure 28 shows global maps of the comparison. The results for AATSR are shown on the left and the results for Metop-A are shown on the right. The first row shows ECHAM data collocated with the satellite swath. The second row the satellite data and the third row the difference between satellite and model.

The following general observations are made

1. At first glance the maps of global differences for each satellite show similar spatial biases, positive biases ( i.e higher model AOD) in the Saharan dust regions and central African biomass burning region. Negative biases around coastal Asia.
2. A small (triangular shaped) positive bias is seen in both the AATSR and PMAp comparisons to the left of South America following the southern branch of the ITCZ. This region is characterised by low cloud. A possible explanation for this is that the model is not adequately flushing out the precipitation scavenged aerosol (i.e. lack of deposition) and/or too much sea salt.
3. There is significant cloud contamination in the AATSR product located on the west coast of the United States. This region has a small number of collocations however the cloud masking should be revised for this region.
4. A large dust event is captured in both model and satellite data

A select number of regions are examined in further detail.

Figure 32 and Figure 33 show the comparison between AATSR and Metop-A for the Saharan dust region close and far from the coast respectively. Note that although nominally the same month the swath collocation for AATSR compared with Metop-A with the model was sensitive to different features in the model this is to be expected because of the different swaths, crossing times and strong temporal features of the dust plume observed. Both satellites show similar features, differences are most likely due to differences in cloud masking from the daily comparison Metop-A appears to capture the dust event very well.

Figure 31 Compares the Metop-A and AATSR clean open Southern Indian ocean region. While the AATSR results show closer agreement with the model. It is not possible to exclude cloud contamination as a factor in increasing the averaged aerosol optical depths over sea and in fact the Metop-A values may be correct.

### 3.5.1. DETAILED DISCUSSION ON DIFFERENCES BETWEEN MODEL AND SATELLITE BIOMASS BURNING

The Central African biomass region of high AOD is interesting for a number of reasons including local air quality, and the effects of the AOD on climate either through effects on clouds in the region or the impact on TOA radiative fluxes. Hence it would be desirable to obtain some closure on the accuracy of the satellite data or model. Unfortunately there is very little ground truth data in this region to verify in a statistical sense the accuracy of either product.

The AATSR data confirms the differences seen between Metop-A retrievals and the model. As part of the Aerosol CCI program, analysis has been performed to understand the effectiveness of the cloud masking and the effect of selecting aerosol type and this is included here for useful background information.

The model uses daily GFAS emission data for wildfires which themselves are derived from fire counts measurement by satellite. Comparisons with MODIS result in very good agreement over both Amazon and Central Africa, however the method for converting fire counts to emissions is complex and an active area of research and reevaluation.

Satellite retrievals of aerosol in this region are complicated by a number of factors including high cloud fraction and a mixture of aerosol types that are both scattering and absorbing. High aerosol amounts can be falsely identified as cloud, biasing the satellite observed values low. Figure 34 shows a comparison of AATSR collocated Cloud and Aerosol products retrieved using the ORAC algorithm but applying different clouds masks which have been optimised for detecting either cloud or aerosol respectively. The red regions in the bottom plot indicate where no cloud or aerosol retrieval was made. Central Africa is one of the most uncertain regions. The Saharan dust outflow is also clearly fully observed. Note the aerosol cloud mask used in this data set was one of the least conservative masks used in the project ( i.e detects the most aerosol) . Figure 35 Fire counts for the period of June/July/August from the paper by G. Roberts et al on annual African biomass burning temporal dynamics. The region of highest fire counts corresponds to this large missing region suggesting that this satellite algorithm (and others as well) has trouble distinguishing smoke from clouds. Which would lead to an underestimation of biomass aerosol in this region. Note that the largest uncertainty is over land and is not as significant over sea.

The patterns of high aerosol loadings and the differences with the model are similar for both AATSR and PMAP see Figure 28. Figure 29 and Figure 30 compare AATSR and Metop-A for the region in more detail, as in the previous section high aerosol peaks are missing in both satellite data sets. Both comparisons suggest the satellites underestimate aerosol loading or the model predicts too much aerosol.

In order to shed more light on the area two more data sets were introduced to provide extra information. The OMI AAI ( Aerosol Absorbing Index) for June 2010, see Figure 36, and the CCI Polder data set, unfortunately the Polder product is only available for a single year so the global map is for July 2008.

The TOMS / OMI aerosol absorbing index is a measure of how much the wavelength dependence of backscattered UV radiation from an atmosphere containing aerosols (Mie scattering, Rayleigh scattering, and

absorption) differs from that of a pure molecular atmosphere (pure Rayleigh scattering). Quantitatively, the aerosol index AAI is calculated from the ratio of measured to calculated 360 nm TOMS / OMI radiances. Under most conditions, the AAI is positive for absorbing aerosols and negative for non-absorbing aerosols (pure scattering). Because the AAI is calculated from the difference in reflectance at two UV wavelengths, it is not possible to directly relate it to a single aerosol quantity [de Graaf et al.2005 However it has been compared to AERONET ground-based measurements to show that the AI tracks the measured optical depth. The AAI value is sensitive to the height of the aerosol plume. [<http://andromeda.caf.dlr.de/satellite-aerosol-products/tomsomi-absorbing-aerosol-index>]

The spatial patterns of AOD from AATSR and PMAp are consistent with the AAI ( Aerosol Absorbing Index) provided by the OMI product. However given the non linear relationship between AAI and AOD no concrete conclusion can be made. The Polder product is also consistent with Metop-A in the biomass region, note also that the AOD values over the southern ocean are more consistent with Metop-A then the model.

The optical properties used in the retrieval are clearly an important factor in evaluating this region. Figure 37 shows the effect of selecting different aerosol types. The plot on the left shows the finemode AOD at 550nm when the aerosol type was selected as the one that resulted in the lowest cost for the retrieval, the plot on the right uses the AeroCom model mean to define the aerosol type. The optical depths differ significantly a indication of the high sensitivity to optical properties.so it could be a significant factor in the differences. For future work the authors suggest in order of increasing effort.

1. Examining the optical properties used in the retrieval and comparing with the model species.
2. Evaluating the sensitivity of the retrieved AOD to the selection of optical properties. This could be easily achieved by performing the same retrieval for different aerosol types and looking at the channel residuals.
3. A more conclusive comparison would be to forward model the model variables into radiance space and compare with the satellite radiances directly. Such a technique although complicated would confirm if the model burdens are well predicted.

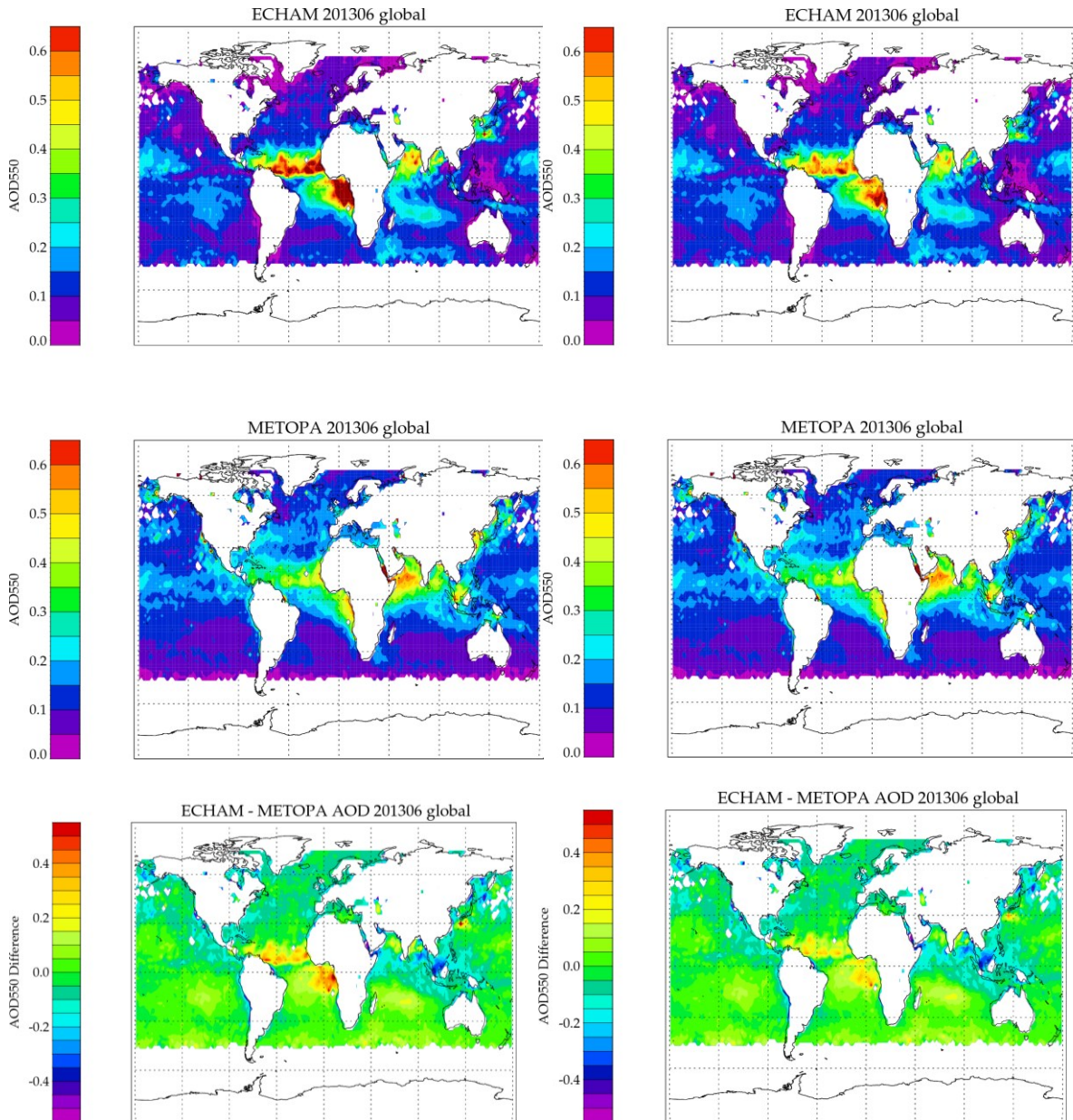


Figure 27 Comparison of model (top) and satellite data (middle) for all possible collocations (left) and for collocations where the model AOD > 1.0 have been removed (right). The difference plots between the model and satellite AOD for the original (left) and the model with AOD > 1.0 removed (left) is shown on the bottom row.

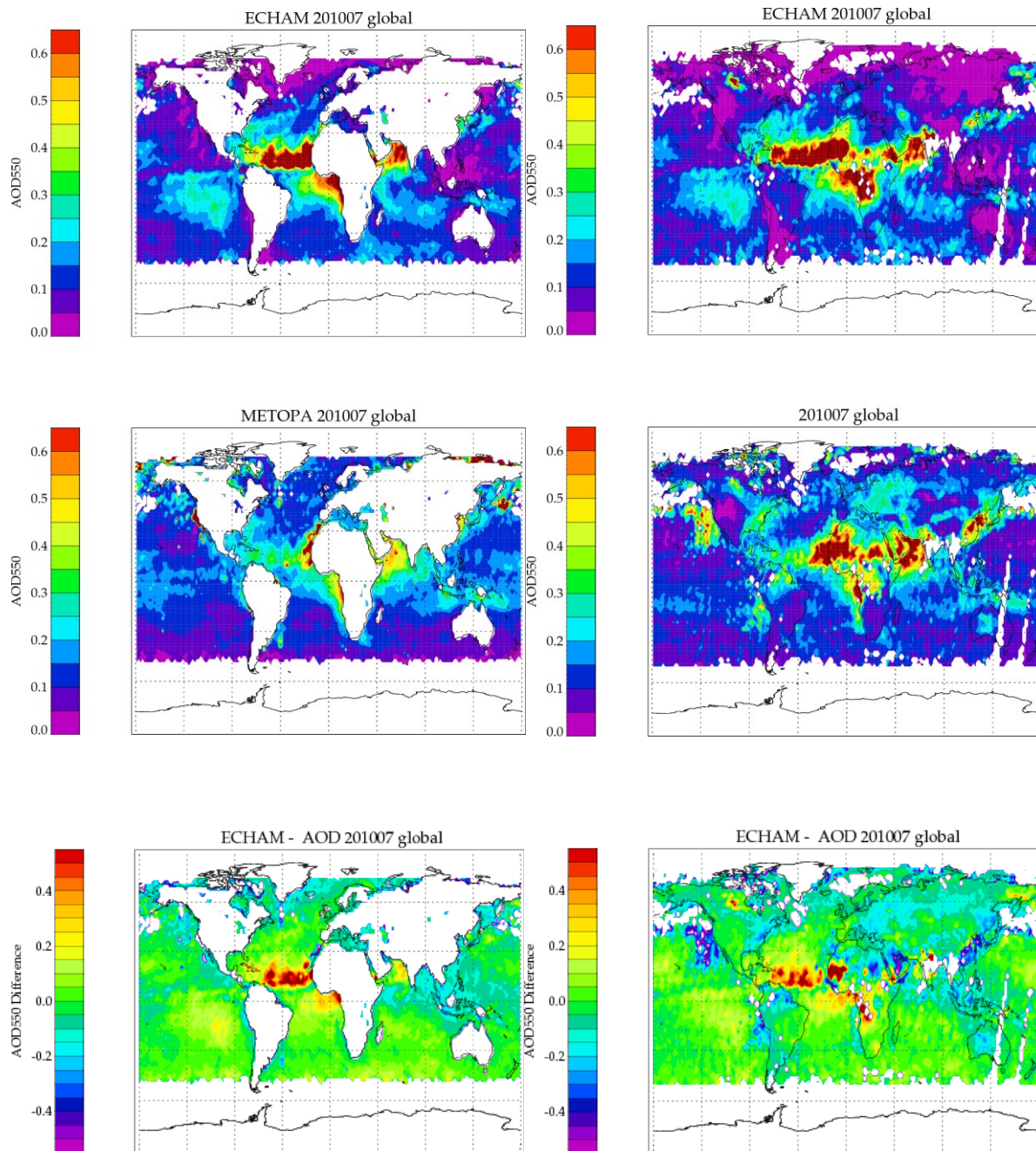


Figure 28 Comparison of June 2010 ECHAM (top row) Metop-A (middle left) and CCI ORAC AATSR ( middle right) the difference between satellite and model results are shown on the bottom row.

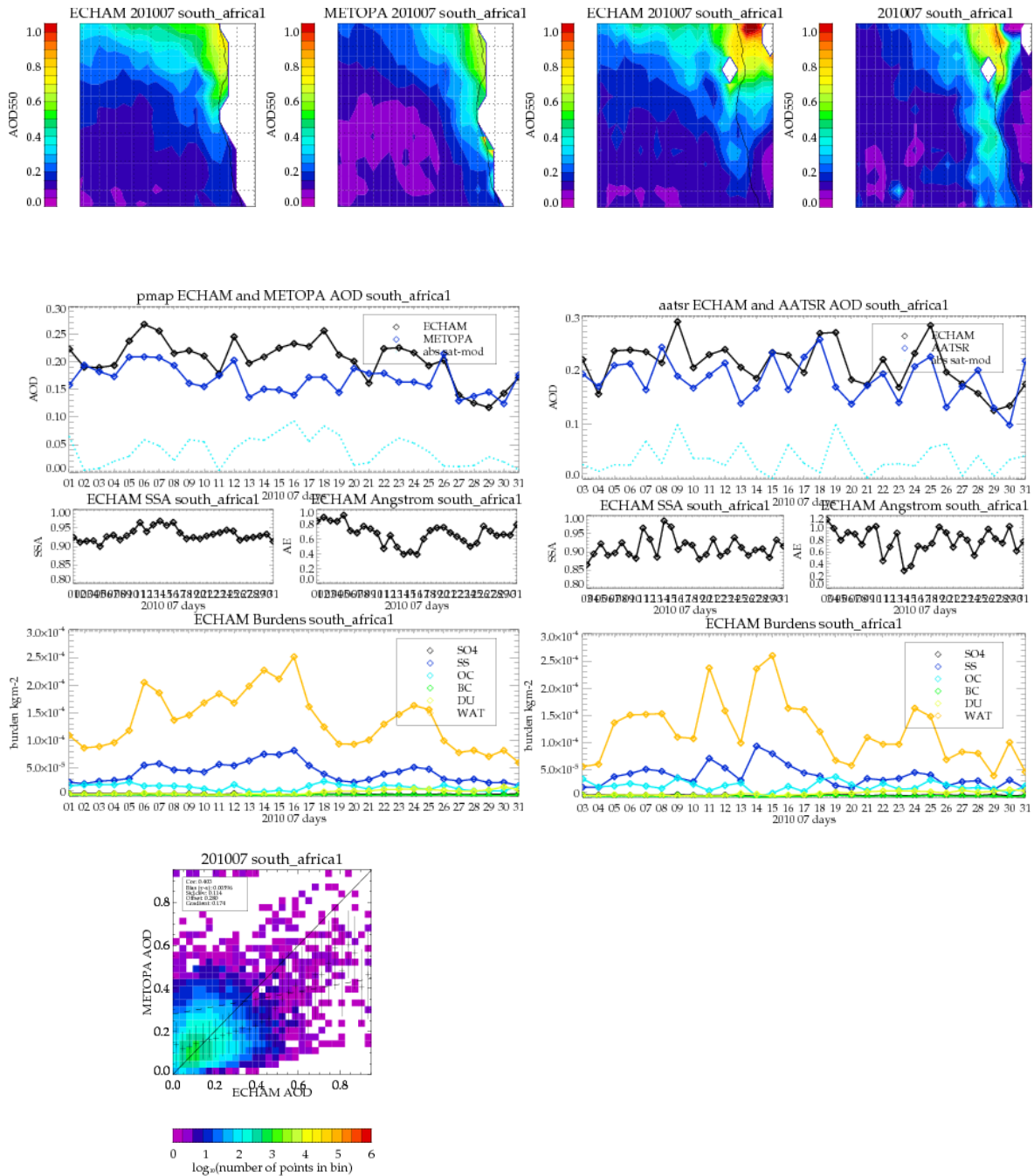


Figure 29 Comparison of Metop-A (left) and AATSR (right) African Biomass burning regions south of the equator for July 2010.

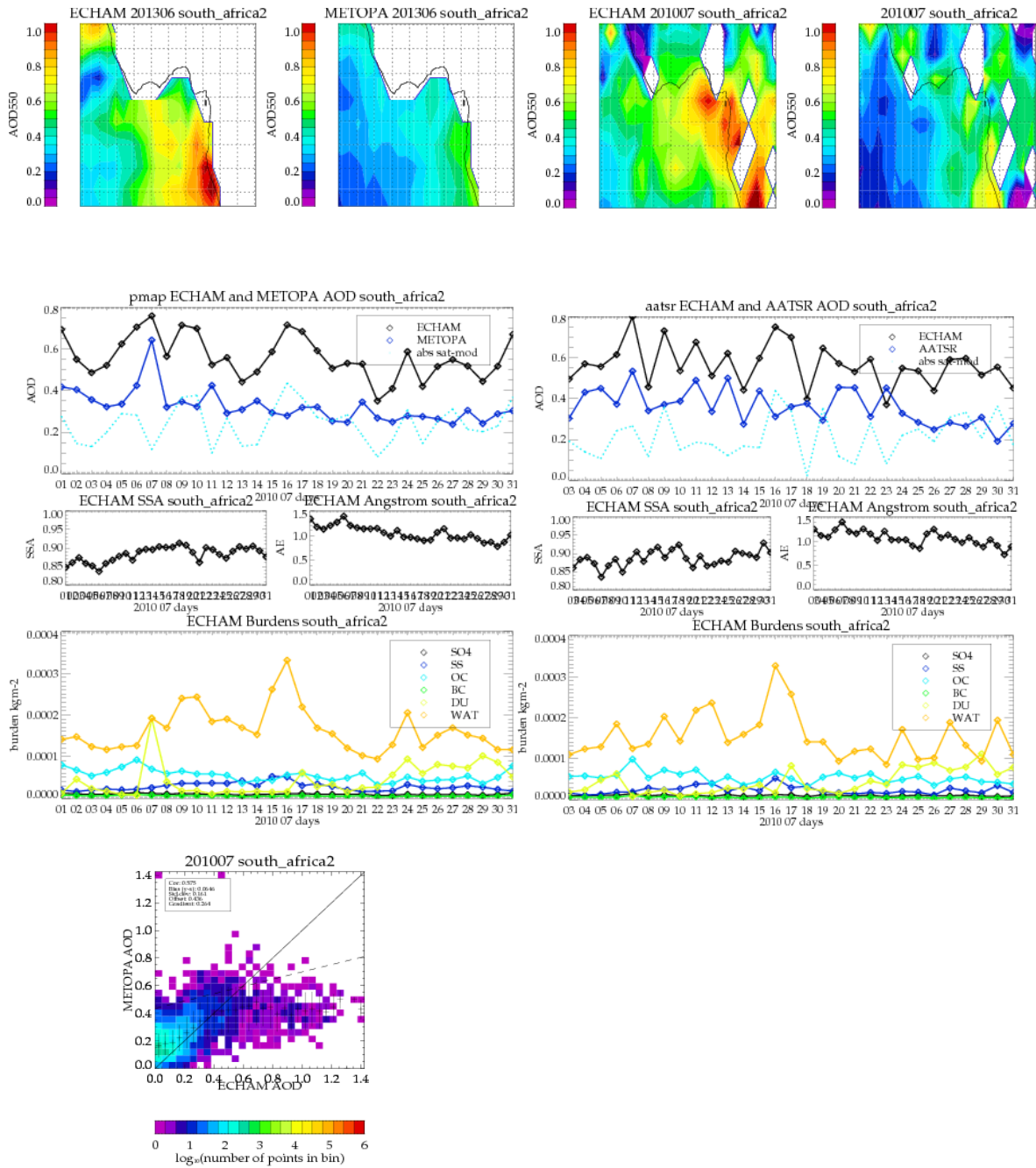


Figure 30 Comparison of Metop-A (left) and AATSR (right) African Biomass burning regions north of the equator for July 2010

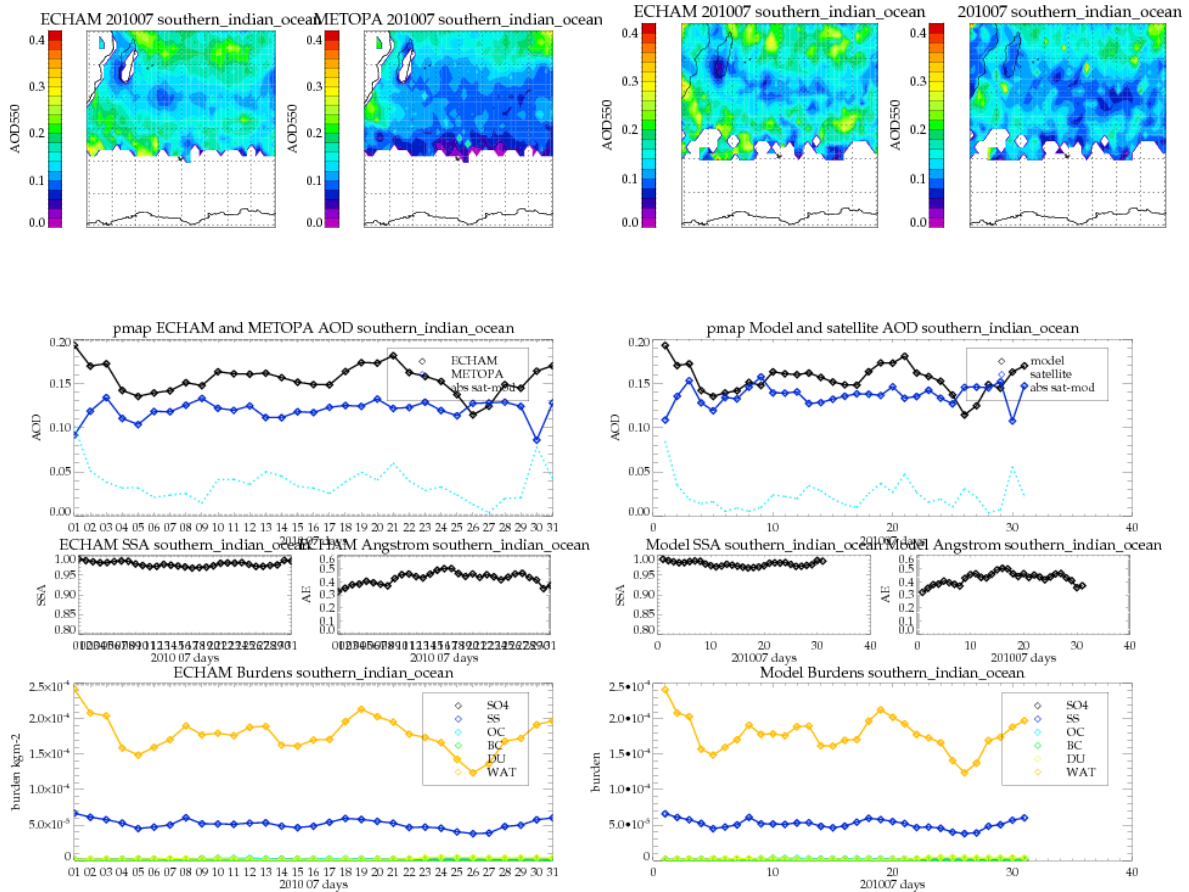
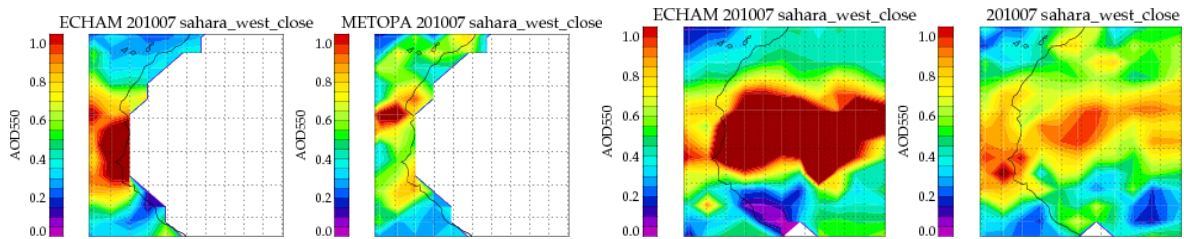


Figure 31 Comparison of Metop-A (left) and AATSR (right) and Southern India for July 2010.



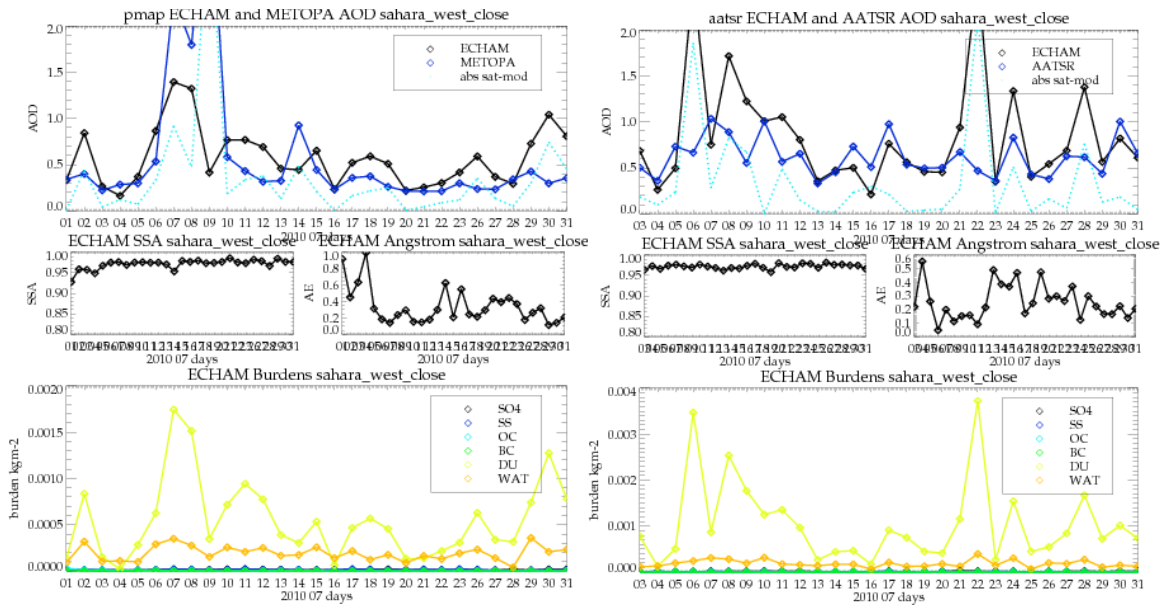
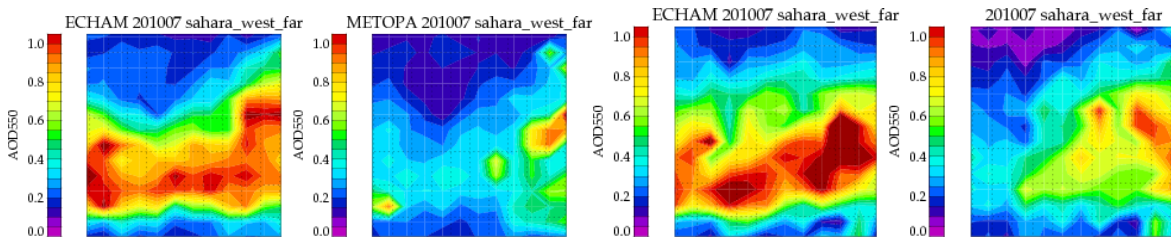


Figure 32 Comparison of Metop-A(left) and AATSR(right) Saharan dust close to the coast for July 2010.



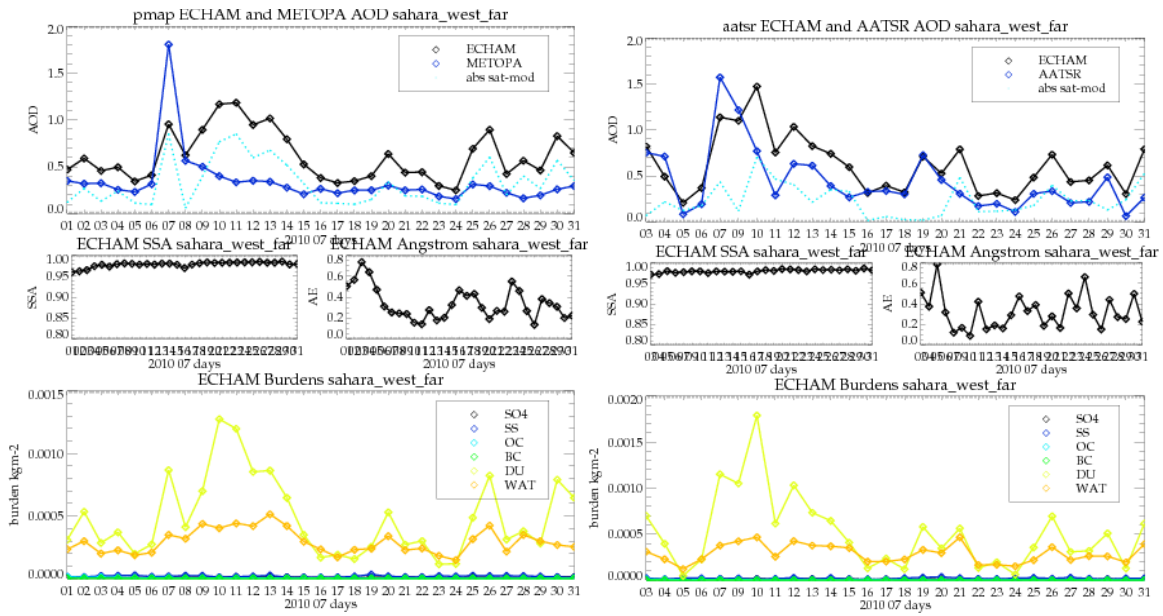


Figure 33 Comparison of Metop-A(left) and AATSR(right) Saharan dust far from the coast for July 2010.

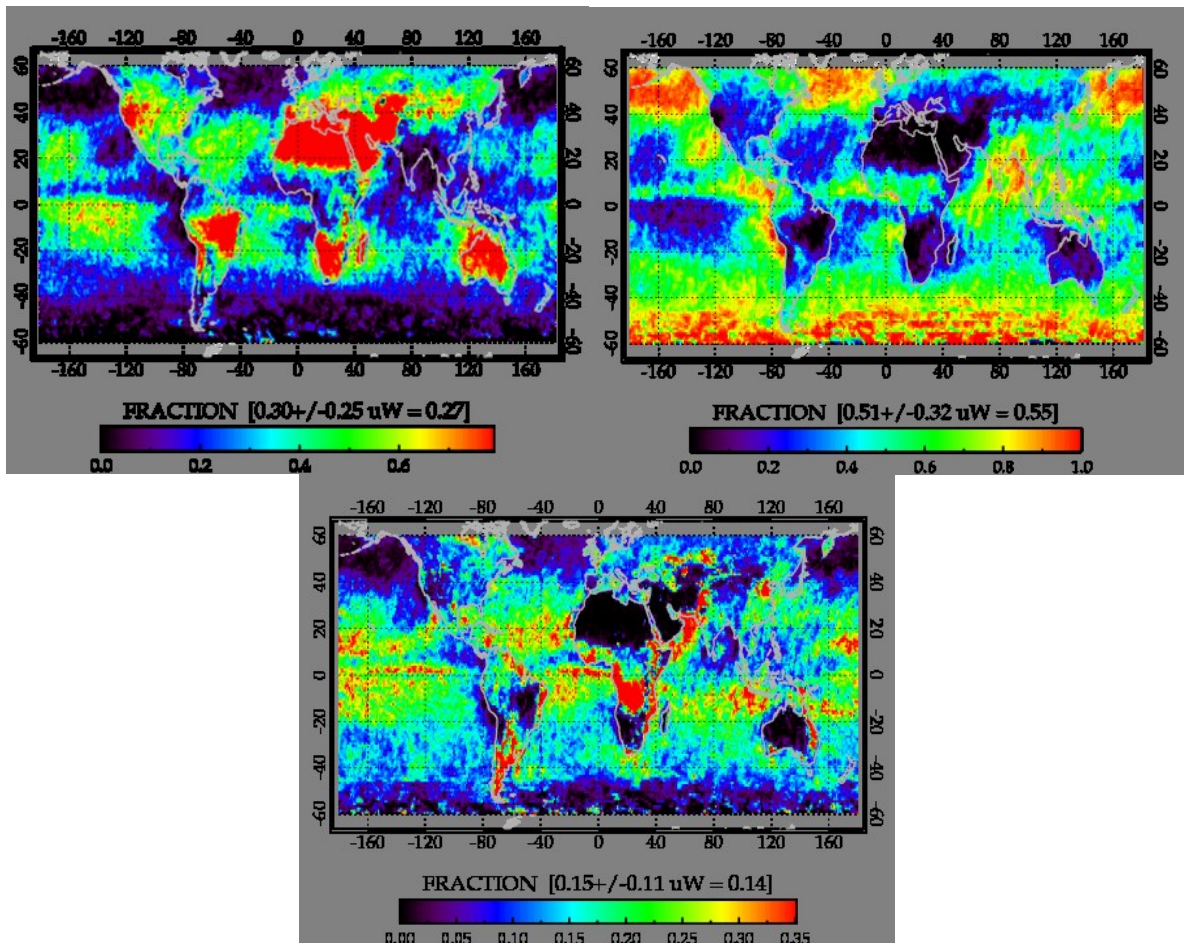


Figure 34 Analysis of AATSR cloud mask using Aerosol CCI and Cloud CCI products for June/July/August 2008. Top left shows the Aerosol CCI clear (aerosol fraction), top right shows the cloud fraction, and the bottom plot shows where the pixel is not classified either clear or cloudy.

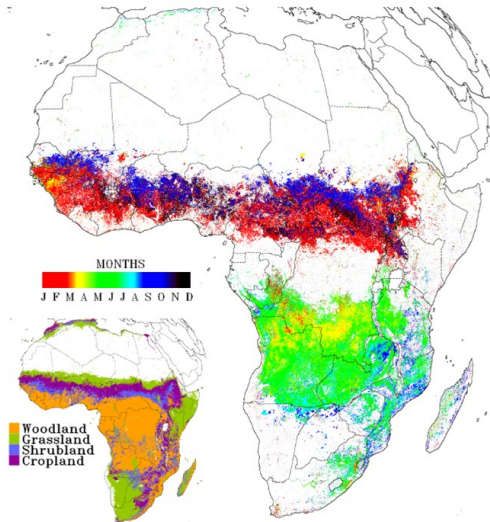
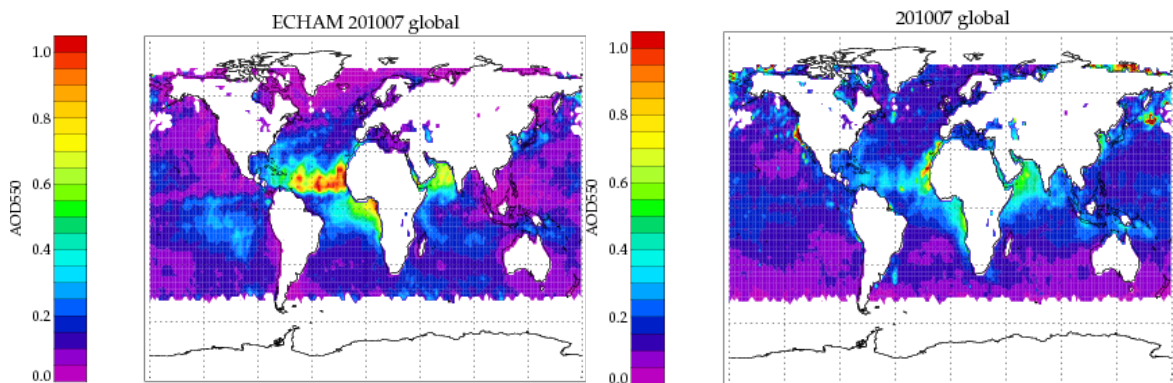


Fig. 1. Geostationary active fire detections over Africa for 2004, colored by day of detection. Multiple fires in the same grid cell are given the date of the last 2004 burning event. Inset map: Global Land Cover 2000 land cover map aggregated into four broad land cover classes.

Figure 35 Fire counts for the period of June/July/August from the paper by G. Roberts et al on annual African biomass burning temporal dynamics.



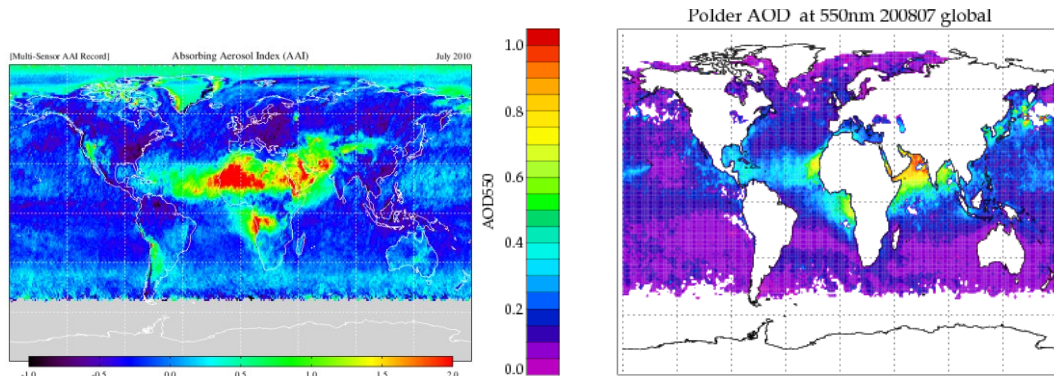


Figure 36 Top row: June 2010 MODEL AOD and Metop-A AOD, bottom row: June 2010 OMI AAI (Courtesy KNMI) and CCI Polder AOD July 2008

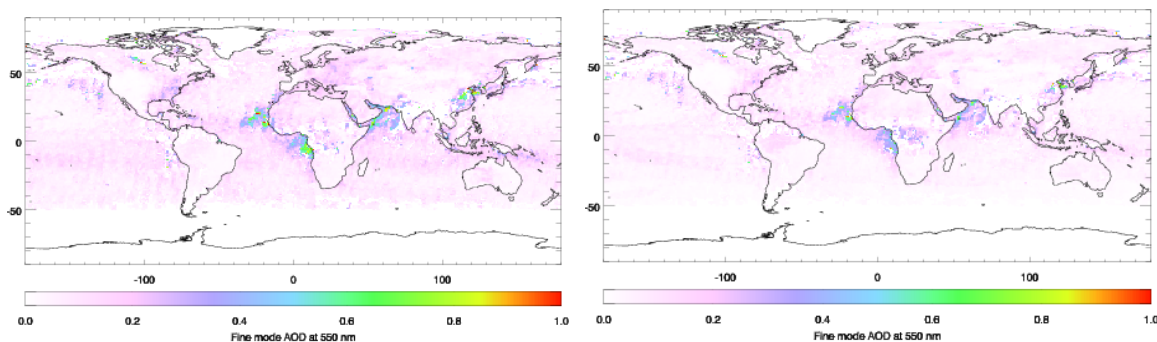


Figure 37 Fine Mode AOD for AATSR for July 2010 'lowest cost' type on the left and AEROCOM model aerosol type on the right.

### 3.6. COMPARISON WITH AERONET DATA

A number of primarily island Aeronet sites were provided that could provide collocations that were representative of retrievals over ocean for both the satellite and Model. The collocation was performed at model grid resolution. Only one site, Dakar, provided any collocations see Figure 38. The findings are not very conclusive or statistical with both model and satellite showing agreement and disagreement with Aeronet depending the day, interestingly the collocation on June 20<sup>th</sup> which predicts an AOD >1 in the model supports the analysis in the previous section that the model is producing too much dust. Despite the inconclusive result in this case. Triple collocations should form a key aspect of model/satellite comparison over land where the number of collocations will be much improved.

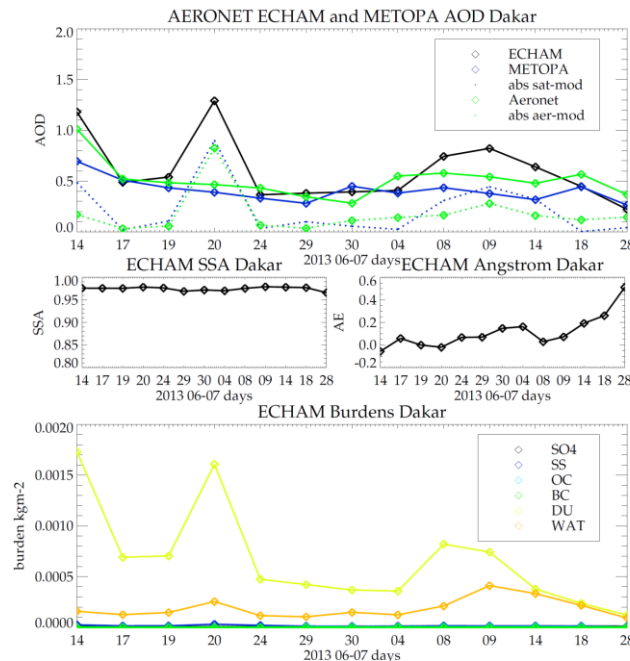


Figure 38 Triple collocation of Model, satellite (Metop-A) and Aeronet for June and July 2013.

### 3.7. RESULTS OF CASE STUDY: LARGE EUROPEAN DUST EVENT MARCH/APRIL 2014.

In late March and early April 2014 Europe experienced one of the year's worst smog and dust pollution events starting in southern Europe and extending all the way to Southern England following a combination of strong winds and powerful dust storms in the Sahara that resulted in fine red dust deposited on the streets of Europe. Figure 39 show an air pollution warning and some images from Southern England. If satellites are able to observed extreme pollution events such as these then assimilation of the data into Models such as are operated at the European centre for the Copernicus Atmosphere Service could improve the prediction capabilities of regional models. Figure 40 shows the false colour pink imagery from the SEVIRI instrument for the 29<sup>th</sup> of March. The thick dust plume (bright pink) is clearly visible. Also visible is a large bank of thick cloud (red) which accompanied the aerosol plume for many days.

ECHAM's main focus is not air quality forecasting and not much effort has been done for validating dust outbreaks over Europe due to transport from Africa. Despite this the model manages quite well to simulate Saharan dust close to its sources.

Figure 41 shows the global maps of aerosol AOD over Europe for the end of March and the beginning of April. The Aerosol plume is clearly visible in the satellite data with average values typically 0.4. The plume is clearly seen in the model data and is associated with a significant dust component in the aerosol over Europe. The time series suggests it is underestimating the AOD by approx. a factor 2 in some locations. While there were no good Aeronet coincidences with the Metop data, probably due to the high cloud coverage during the period. Values measured at the Oostende Aeronet station on the days of the dust storm are consistent with

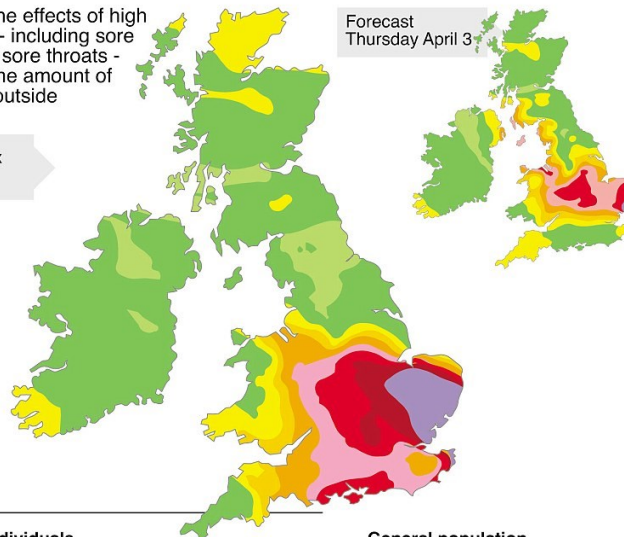
the values measured by the satellite see Figure 43. Given the high cloud coverage during this period the satellite data performs well in able to distinguish the extreme dust event.

### UK air pollution warning

People suffering the effects of high levels of pollution - including sore eyes, coughs and sore throats - should cut down the amount of activity they take outside

Daily air quality index  
 Wednesday April 2

Forecast  
 Thursday April 3



### Health advice

#### At risk individuals

- 1 2 3 Low:** Enjoy your usual outdoor activities
- 4 5 6 Moderate:** Adults and children with lung problems, and adults with heart problems, who experience symptoms, should consider reducing strenuous physical activity, particularly outdoors
- 7 8 9 High:** Adults and children with lung problems, and adults with heart problems, should reduce strenuous physical exertion, particularly outdoors, and particularly if they experience symptoms. People with asthma may find they need to use their reliever inhaler more often. Older people should also reduce physical exertion.
- 10 Very high:** Adults and children with lung problems, adults with heart problems, and older people, should avoid strenuous physical activity. People with asthma may find they need to use their reliever inhaler more

#### General population

Enjoy your usual outdoor activities

Anyone experiencing discomfort such as sore eyes, cough or sore throat should consider reducing activity, particularly outdoors

Press Association Graphic

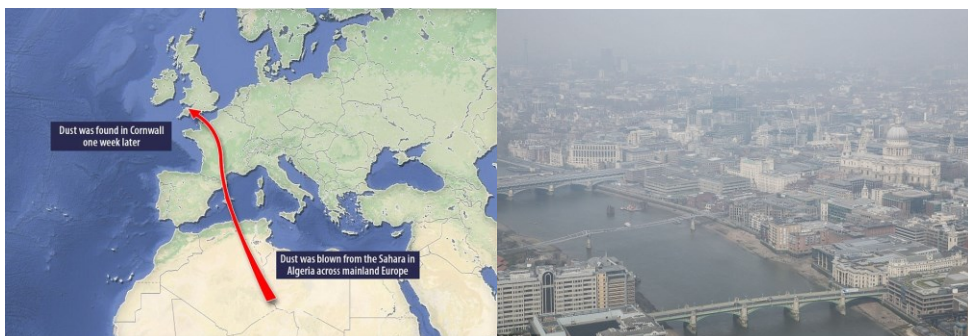


Figure 39 Pictures from UK newspapers indicating the seriousness of the March/ April Saharan dust event.

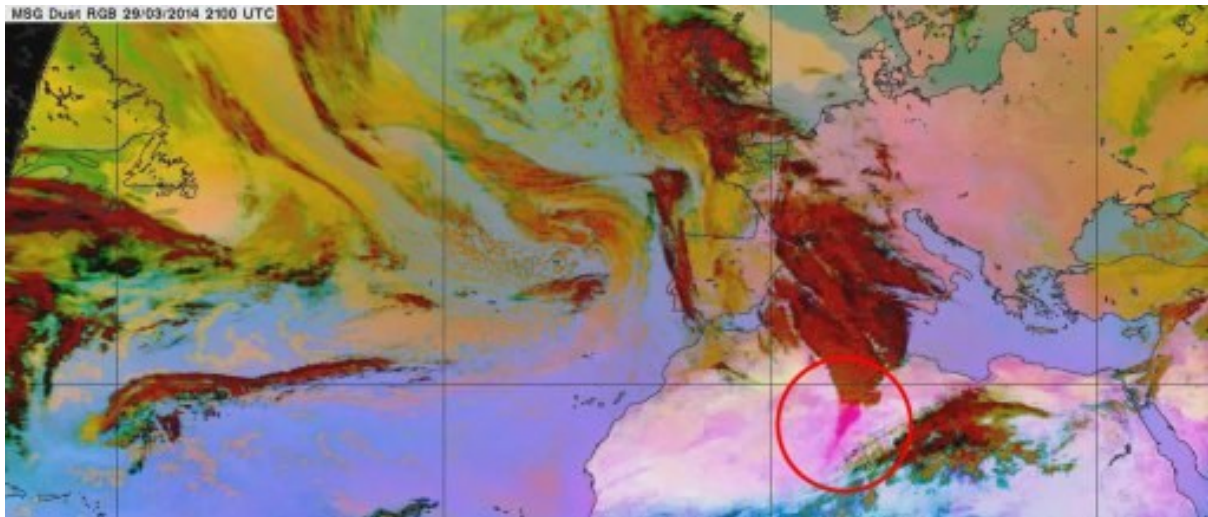
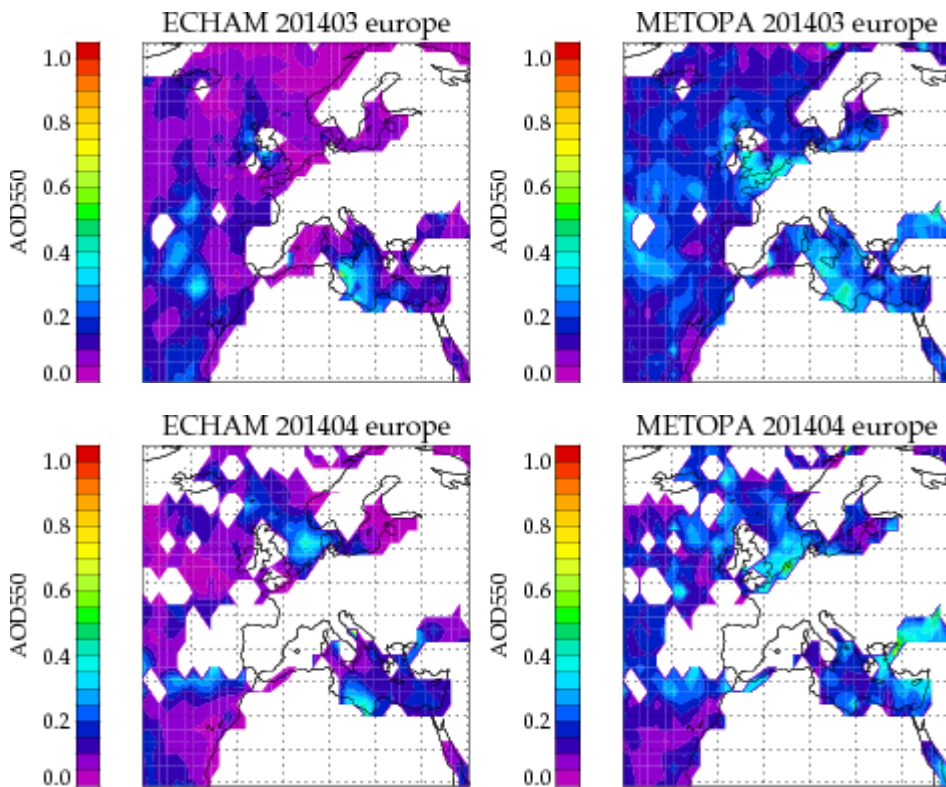


Figure 40 March 29th 2014 SEVIRI dust image (dust plume can be seen in pink, clouds are indicated in dark red)



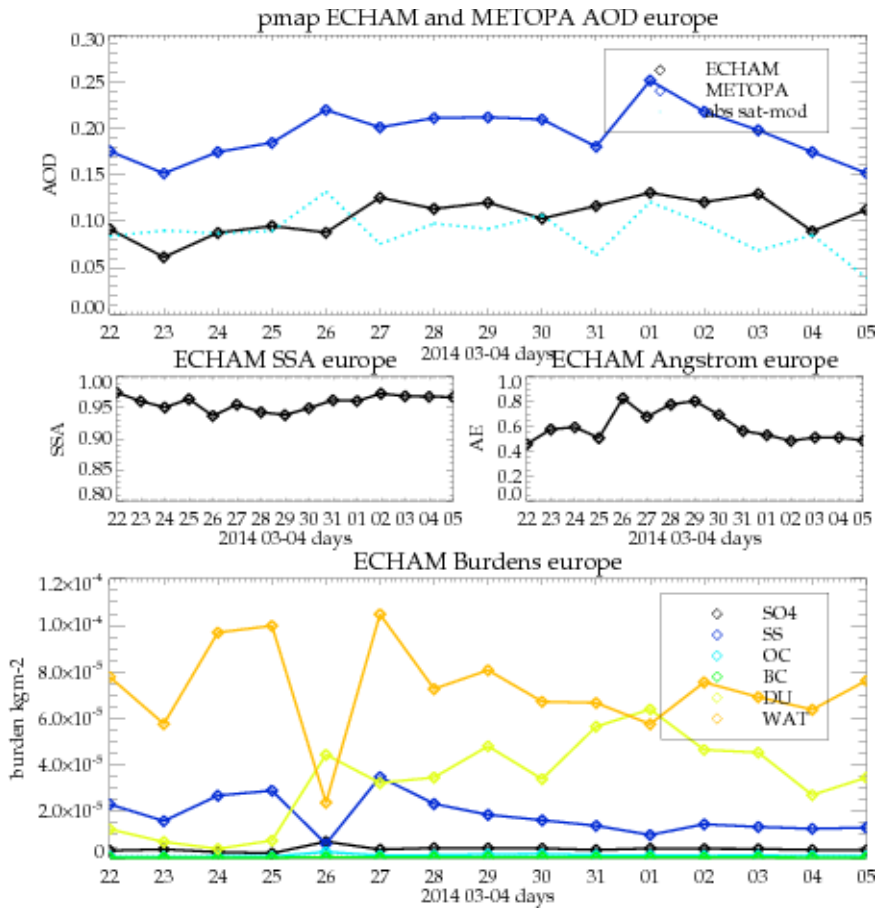
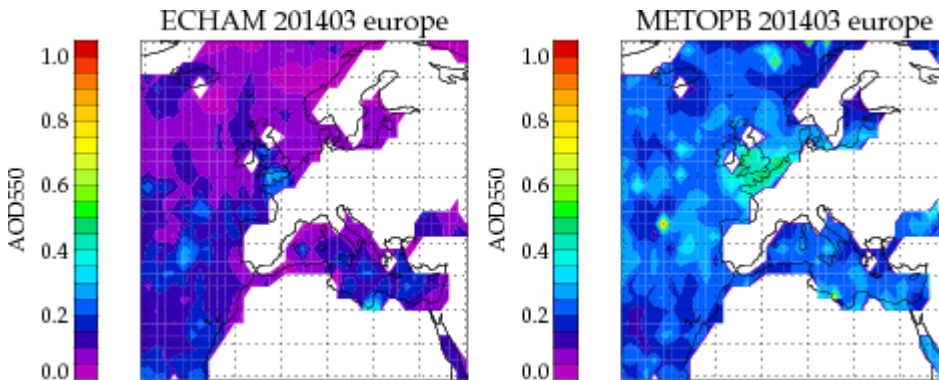


Figure 41 ECHAM and Metop-A comparison over Europe for March 23<sup>rd</sup> to April 5<sup>th</sup>. Top plot shows regional comparison, middle and bottom plots shows time series of model and satellite daily collocations.



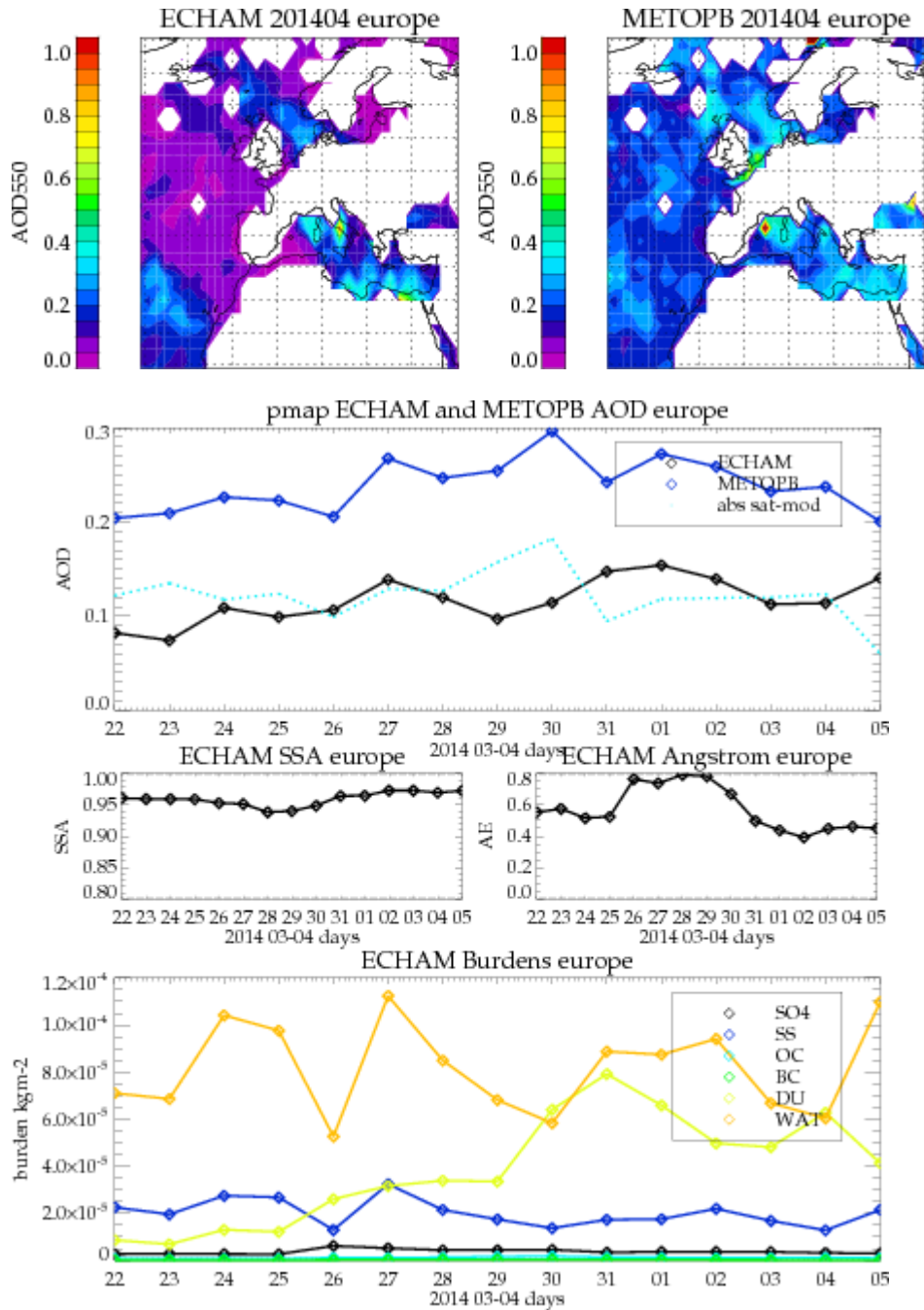


Figure 42 ECHAM and Metop-B comparison over Europe

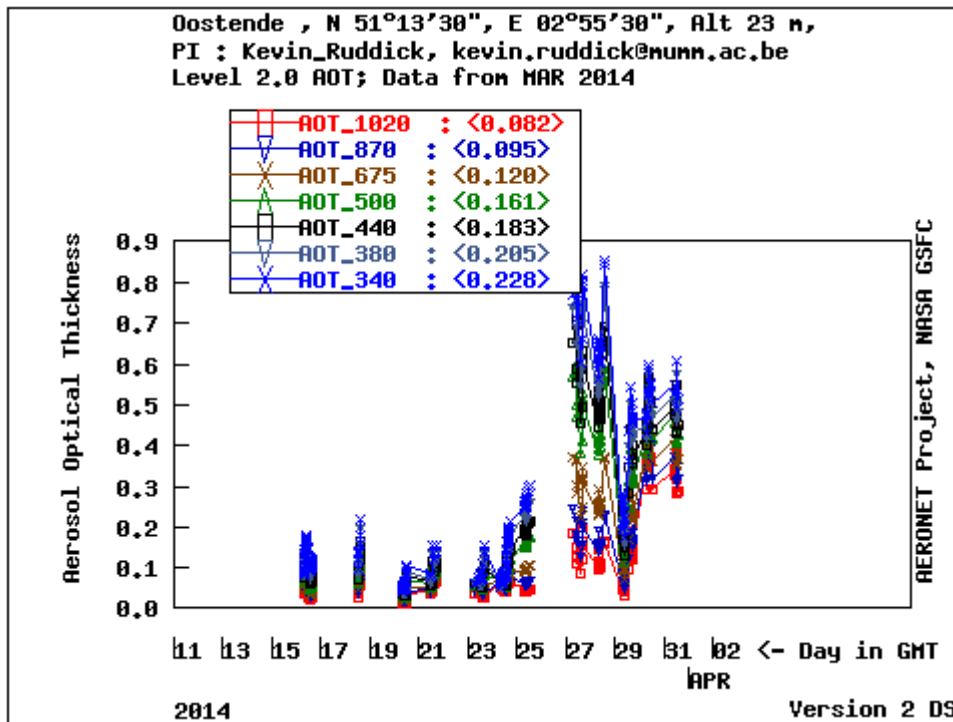


Figure 43 Oostende Aeronet station results March/April 2014

## 4. CONCLUSIONS

Overall the Metop-PMAp aerosol products show good agreement with the ECHAM model with a few key differences.

Typically satellite observations are used to validate models and this study has been useful in that aspect providing useful feedback to the ECHAM modelling community. While comparisons with Aeronet data should be the prime source of validation for satellite aerosol products comparisons with model data are useful exercises as they provide full global coverage and are unaffected by the effects of cloud identification. Aeronet/satellite comparisons can be biased because they cover mainly land regions and areas such as Africa, Asia, Russia and polar regions have sparse coverage. Furthermore Aeronet/satellite comparisons are usually only performed for a strict criteria where Aeronet and satellite observations are assumed to be clear and not affected by cloud. Evidence is now gathering that Aeronet might be too strict in the cloud masking used in the level 2.0 product leading to a negative bias in true aerosol amounts. Model comparisons can shed light on this bias.

The Metop-B AOD retrievals were found to be positively offset compared with Metop-A as has been observed in other analysis. This raises the important effect of calibration on aerosol retrievals and the authors suggest

that more attention be given to this aspect before the next reprocessing. This could be especially complicated for this algorithm as two instruments (and possibly more in the future) are involved and it is important to consider compensating effects in the calibration.

Over polluted areas (Europe and East-Asia), the model AOD is always too low although there is a strong temporal and spatial correlation between model and observations. The underestimation is likely due to the absence of nitrate as aerosol in the model and the rather unsophisticated treatment of VOCs (Volatile Organic Compounds) and their resulting SOA (Secondary Organic Aerosol).

The months selected (June/July 2013) captured the emissions from extensive forest fires in Canada. The increased aerosol emissions were captured in both the model and satellite, although the magnitude and distribution differed. The satellite AOD was consistently higher than the model AOD except at the beginning of biomass event.

Modelled wildfire in the Amazon and Savannah agrees rather well with MODIS AOD but in Siberia and boreal America there are significant differences in both timing and magnitude of wildfire events. Notably, modelled (and MODIS-observed) AOD due to wildfires in boreal America are usually much lower than that in the Amazon. This in turn is due to lower emissions. These emissions come from the GFAS database that includes estimates of SO<sub>2</sub>, BC and POM emissions from MODIS observed fire radiative power. We surmise that smaller, more disperse and low intensity fires would be harder to observe than major fires.

The comparison with the Western Saharan dust plume indicated that the PMAp retrieval could be screening very high aerosol events typically events with AOD >1. This effect was particularly apparent close to the coast and decreased in magnitude down stream. While this region has been well studied by ECHAM modellers and independent model/Aeronet comparisons show the model having good agreement with Aeronet. There was an indication in the model/Aeronet comparison that the values observed in the months of June and July are over estimated by the model. This overestimation was also observed in the model/satellite comparison. On a number of days the model results 'spiked' to values > 1.0 on these particular days the model and PMAp product disparity was largest. Individual inspection of MSG dust imagery on these days did not suggest the presence of strong aerosol episodes. The comparison was repeated with the collocations that showed model AOD > 1.0 removed from the collocated data set. The correlation between satellite and model was greatly improved. Globally the model AOD decreased in regions with high aerosol loading the corresponding satellite AOD showed very little change.

East of the Sahara the opposite was observed with the satellite measuring more AOD than the model. The typical AOD values are much lower for this region so cloud screening is less likely to be a problem. Estimating dust emissions in the model is complicated and relies on accurate identification of sources. It is likely in this case that the satellite observations are good and the model emissions underestimated.

In the regions of open ocean results were complex.

- The monthly standard deviation indicated regions of higher variance in cirrus dominated regions that might suggest the presence of cloud in the PMAp product.

- In the southern ocean PMAp AOD is less than the model, with the model results showing significant variance in time (largely due to water content) compared to the satellite retrievals. The model is known to have too much SS emissions so the satellite estimates may be reasonable.
- In the northern polluted regions the AOD is greater than the model. In this region there are two modelling deficiencies, too much SS emissions over water in general but not enough polluted aerosol. This region is further complicated by dust and in the months investigated in this report a significant biomass event occurred.

Significant differences in the model and satellite biomass aerosol optical depths was observed in the Central Africa/Sahel region, extra data sets were brought in to provide insights into the differences. This is a region of active research in both the model and satellite communities and hence the uncertainty in this region is high. Unfortunately there is little ground based data to provide an accurate validation source. The results were analysed as a function of two different regions above and below the equator.

The African region below the equator showed good spatial correlation between model and satellite except the satellite data extended further south than the model. The Model predicted significantly more aerosol. The AATSR CCI retrievals confirmed a similar bias compared to the the model results. This region has a significant component of absorbing aerosol. If the amount of absorption was significantly underestimated in the optical properties used in the satellite retrieval then the retrieved optical depth would be biased low. This uncertainty in optical properties cannot be discounted although it is probably not the cause of all the bias.

The Sahel region above the equator is more complex with a mix of dust and absorbing carbon aerosols and high relative humidity. This region shows more significant bias. Either the model overestimates the amount of absorbing type aerosol or water vapour absorption or the satellite does not assume enough absorbing aerosol. A more sophisticated forward modelling of model burdens into radiance space could provide illumination in this region.

The Aerosol CCI AATSR data set confirmed most of the same satellite differences in the model although the cloud screening was slightly less conservative, this resulted in some residual cloud contamination in the CCI data. This data also highlighted the likelihood of differences due to cloud screening and assuming an incorrect aerosol type via extra analysis that has been performed on this data.

The PMAp algorithm demonstrated skill above the model in observing the extreme dust events that blanketed Europe in March April 2014 even when the region was blanketed with significant cloud cover. It would be interesting to conduct a assimilation experiment for this event to see if it enhanced air quality prediction skill.

The authors are confident that with the current accuracy of the PMAp product the product will be of value to users, and modellers for future analysis.

#### 4.1. FURTHER WORK AND RECCOMENDATIONS

Aerosol retrievals are sensitive to an instruments calibration, before another reprocessing the calibration of the instruments should be investigated and applied.

A small subset of Island Aeronet sites was used in this study. For a statistical analysis of the few months this was not sufficient. The Aeronet comparison should be extended to cover coastal regions.

One of the most intriguing regions was the Central African biomass region unfortunately has no Aeronet ground based validation. Can EUMETSAT promote the installation of additional Aeronet stations in the Central African biomass region or support campaigns in this region?

The optical properties used in the satellite algorithms can significantly affect the retrieved AOD. Considerable uncertainty for absorbing aerosols exists. The following tasks would be beneficial to both model and satellite analysis

- a. Examine in more detail the optical properties used in the retrieval and compare them with the model types.
- b. Evaluate the sensitivity of the retrieved AOD to the selection of optical properties. This could be easily achieved by performing the same retrieval for different aerosol types and looking at the channel residuals.
- c. A more conclusive comparison would be to forward model the model variables into radiance space

The clean southern oceans show significant differences between most models and satellite data sets to achieve some closure all MAN observations in this region should be analysed, in particular as a function of meteorology.

The model predicts significantly more dust aerosol in the months of June and July. Detailed investigation pin pointed the biggest differences are caused by aerosol spikes on particular days, when these spikes were removed from the analysis the correlation improved. Dust/cloud identification is difficult and while the model clearly needs to investigate these anomalous events. The standard deviation of the satellite AOD retrievals shows variance in some low AOD ocean regions which might be expected to have low aerosol variance. Higher than expected variance could be caused by cloud contamination. Confidence in the algorithm would increase if more validation of the cloud mask was performed by the developers. This could be achieved through statistical comparison (overland) with Synop measurements and Aeronet observations

Another potential source of data to examine cloud masking is the Calipso and Cloudsat instruments. If strict temporal collocation with Calipso/Cloudsat measurements was applied this could also provide useful information on contamination from sub pixel and cirrus clouds, over land and sea.

Processing a whole year of data would be statistically more representative and cover the diurnal cycle of aerosol events as well as improving the MAN & Aeronet coverage.

Finally the PMAp satellite data has usefully shown areas where the model data could be improved. In particular, these two issues stand out: wildfire emissions for boreal America and Siberia are poorly constrained by satellite observations leading in turn to poorly modelled AOT; wet-growth of aerosols due to ambient humidity (and the associated change in optical properties) needs to receive further scrutiny, especially for sea-salt which is the most wettable aerosol in the model.

## 5. REFERENCES

- [Ref:1] Sayer, A. M., Thomas, G. E., Palmer, P. I., and Grainger, R. G.: Some implications of sampling choices on comparisons between satellite and model aerosol optical depth fields, *Atmos. Chem. Phys.*, 10, 10705-10716, doi:10.5194/acp-10-10705-2010, 2010.
- [Ref:2] C. A. Poulsen, P. D. Watts, G. E. Thomas, A. M. Sayer, R. Siddans, R. G. Grainger, B. N. Lawrence, E. Campmany, S. M. Dean and C. Arnold, "Cloud retrievals from satellite data using optimal estimation: evaluation and application to ATSR," *Atmos. Meas. Tech. Discuss.*, vol. 4, pp. 2389-2431, 2011.
- [Ref:3] Miles, G. Ozone profile retrieval from Metop with GOME-2, IASI and AVHRR, Proceedings of the Eumetsat Conference 2012, [http://www.eumetsat.int/website/wcm/idc/idcplg?IdcService=GET\\_FILE&dDocName=PRESENTATIONS\\_SOPOT\\_2012\\_PDF&RevisionSelectionMethod=LatestReleased&Rendition=Web](http://www.eumetsat.int/website/wcm/idc/idcplg?IdcService=GET_FILE&dDocName=PRESENTATIONS_SOPOT_2012_PDF&RevisionSelectionMethod=LatestReleased&Rendition=Web)
- [Ref:4] Siddans, R. C. Poulsen, E. Carboni, Cloud Model for Operational Retrievals from MSG SEVIRI Final Report, Eumetsat Contract EUM/CO/07/460000463/PDW, [http://www.eumetsat.int/groups/ops/documents/document/pdf\\_report\\_cloud\\_model.pdf](http://www.eumetsat.int/groups/ops/documents/document/pdf_report_cloud_model.pdf)
- [Ref:5] R. Siddans, C. Poulsen, Towards Detection and Retrieval of Volcanic Ash from SEVIRI using the OCA Processor, Final Report, EUMETSAT RFQ 10/202688, June 2011
- [Ref:6] Schulz, M., C. Textor, S. Kinne, Y. Balkanski, S. Bauer, T. Berntsen, T. Berglen, O. Boucher, F. Dentener, S. Guibert, I. S. A. Isaksen, T. Iversen, D. Koch, A. Kirkevag, X. Liu, V. Montanaro, G. Myhre, J. E. Penner, G. Pitari, S. Reddy, O. Seland, P. Stier, and T. Takemura (2006), Radiative forcing by aerosols as derived from the AeroCom present-day and pre-industrial simulations, *Atmos. Chem. Phys.*, 6, 5225-5246.
- [Ref:7] Stier, P., J. Feichter, S. Kinne, S. Kloster, E. Vignati, J. Wilson, L. Ganzeveld, I. Tegen, M. Werner, Y. Balkanski, M. Schulz, O. Boucher, A. Minikin, and A. Petzold (2005), The aerosol-climate model ECHAM5-HAM, *Atmos. Chem. Phys.*, 5, 1125-1156.
- [Ref:8] Textor, C., M. Schulz, S. Guibert, S. Kinne, Y. Balkanski, S. Bauer, T. Berntsen, T. Berglen, O. Boucher, M. Chin, F. Dentener, T. Diehl, R. Easter, H. Feichter, D. Fillmore, S. Ghan, P. Ginoux, S. Gong, J. E. Kristjansson, M. Krol, A. Lauer, J. F. Lamarque, X. Liu, V. Montanaro, G. Myhre, J. Penner, G. Pitari, S. Reddy, O. Seland, P. Stier, T. Takemura, and X. Tie (2006), Analysis and quantification of the diversities of aerosol life cycles within AeroCom, *Atmos. Chem. Phys.*, 6, 1777-1813.
- [Ref:9] Zhang, K., D. O'Donnell, J. Kazil, P. Stier, S. Kinne, U. Lohmann, S. Ferrachat, B. Croft, J. Quaas, H. Wan, S. Rast, and J. Feichter (2012), The global aerosol-climate model ECHAM-HAM, version 2: sensitivity to improvements in process representations, *Atmos. Chem. Phys.*, 12(19), 8911-8949 Doi 10.5194/Acp-12-8911-2012.
- [Ref:10] Myhre, G., B. H. Samset, M. Schulz, Y. Balkanski, S. Bauer, T. K. Berntsen, H. Bian, N. Bellouin, M. Chin, T. Diehl, R. C. Easter, J. Feichter, S. J. Ghan, D. Hauglustaine, T. Iversen, S. Kinne, A. Kirkevag, J. F. Lamarque, G. Lin, X. Liu, M. T. Lund, G. Luo, X. Ma, T. van Noije, J. E. Penner, P. J. Rasch, A. Ruiz, O. Seland, R. B. Skeie, P. Stier, T. Takemura, K. Tsigaridis, P. Wang, Z. Wang, L. Xu, H. Yu, F. Yu, J. H. Yoon, K. Zhang, H. Zhang, and C. Zhou (2013), Radiative

forcing of the direct aerosol effect from AeroCom Phase II simulations, *Atmos. Chem. Phys.*, 13(4), 1853-1877 Doi 10.5194/Acp-13-1853-2013.

- [Ref:11] Stier, P., N. A. J. Schutgens, N. Bellouin, H. Bian, O. Boucher, M. Chin, S. Ghan, N. Huneeus, S. Kinne, G. Lin, X. Ma, G. Myhre, J. E. Penner, C. A. Randles, B. Samset, M. Schulz, T. Takemura, F. Yu, H. Yu, and C. Zhou (2013), Host model uncertainties in aerosol radiative forcing estimates: results from the AeroCom Prescribed intercomparison study, *Atmos. Chem. Phys.*, 13(6), 3245-3270 Doi 10.5194/Acp-13-3245-2013.
- [Ref:12] PMAP update presentation by M Grzegorski Oxford University June 2014.
- [Ref:13] Schutgens et al paper in preparation. ACP
- [Ref:14] Polar Multi-Sensor Aerosol Product Validation Report  
EUM/TSS/REP/14/74543810 October 2014.
- [Ref:15] See discussions, stats, and author profiles for this publication at:  
<http://www.researchgate.net/publication/267215024>
- [Ref:16] D. Carrer, X. Ceamanos, B. Six, and J.-L. Roujean, AERUS-GEO: A newly available satellite derived aerosol optical depth product over Europe and Africa, NOVEMBER 2014, DOI: 10.1002/2014GL061707
- [Ref:17] Hess, M., P. Koepke, and I. Schult (1998), Optical Properties of Aerosols and Clouds: The Software Package OPAC, *Bulletin of the American Meteorological Society*, 79 (5), 310-318, doi:10.1175/1520-0477(1998)079
- [Ref:18] Feichter, J., Kjellstrom, E., Rodhe, H., Dentener, F., Lelieveld, J., and Roelofs, G.-j.: SIMULATION OF THE TROPOSPHERIC SULFUR CYCLE IN A GLOBAL CLIMATE MODEL, *Atmospheric Environment*, 30, 1693-1707, 1996.
- [Ref:19] Folini, D. and Wild, M.: Aerosol emissions and dimming / brightening in Europe : Sensitivity studies with ECHAM5-HAM, *Journal of Geophysical Research*, 116, doi:10.1029/2011JD016227, 2011.
- [Ref:20] Horowitz, L. W., Walters, S., Mauzerall, D. L., Emmons, L. K., Rasch, P. J., Granier, C., Tie, X., Lamarque, J.-F., Schultz, M. G., Tyndall, G. S., Orlando, J. J., and Brasseur, G. P.: A global simulation of tropospheric ozone and related tracers: Description and evaluation of MOZART, version 2, *Journal of Geophysical Research*, 108, doi:10.1029/2002JD002853, 2003. Lin, S.-J. and Rood, R. B.: Multidimensional flux-form semi-Lagrangian transport schemes, *Monthly Weather Review*, 124, 2046-2070, 1996.
- [Ref:21] Lohmann, U., Stier, P., Hoose, C., Ferrachat, S., Kloster, S., Roeckner, E., and Zhang, J.: Cloud microphysics and aerosol indirect effects in the global climate model ECHAM5-HAM, *Atmospheric Chemistry and Physics*, 7, 3425-3446, doi:10.5194/acp-7-3425-2007, <http://www.atmos-chem-phys.net/7/3425/2007/>, 2007.
- [Ref:22] Kazil, J., Stier, P., Zhang, K., Quaas, J., Kinne, S., O'Donnell, D., Rast, S., Esch, M., Ferrachat, S., Lohmann, U., and Feichter, J.: Aerosol nucleation and its role for clouds and Earth's radiative forcing in the aerosol-climate model ECHAM5-HAM, *Atmospheric Chemistry and Physics*, 10, 733-752, doi:10.5194/acp-10-10733-2010, <http://www.atmos-chem-phys.net/10/10733/2010/>, 2010.
- [Ref:23] Kloster, S., Dentener, F., Feichter, J., Raes, F., Aardenne, J. V., Roeckner, E., Lohmann, U., and Stier, P.: Influence of future air pollution mitigation strategies on total aerosol radiative forcing, *Atmospheric Chemistry and Physics*, 8, 6405-6437, 2008.
- [Ref:24] Makkonen, R., Asmi, A., Korhonen, H., Kokkola, H., Järvenoja, S., Räisänen, P., Lehtinen, K. E. J., Laaksonen, A., Kerminen, V.-M., Järvinen, H., Lohmann, U., Bennartz, R.,

Feichter, J., and Kulmala, M.: Sensitivity of aerosol concentrations and cloud properties to nucleation and secondary organic distribution in ECHAM5-HAM global circulation model, *Atmospheric Chemistry and Physics*, 9, 1747–1766, doi:10.5194/acp-9-1747-2009, <http://www.atmos-chem-phys.net/9/1747/2009/>, 2009.

- [Ref:25] Niemeier, U., Timmreck, C., Kinne, S., Rast, S., Self, S., Place, D., and Keynes, M.: Initial fate of fine ash and sulfur from large volcanic eruptions, *Atmospheric Chemistry and Physics*, 9, 9043–9057, 2009.
- [Ref:26] O'Donnell, D., Tsigaridis, K., and Feichter, J.: Estimating the direct and indirect effects of secondary organic aerosols using ECHAM5-HAM, *Atmospheric Chemistry and Physics*, 11, 8635–8659, doi:10.5194/acp-11-8635-2011, <http://www.atmos-chem-phys.net/11/8635/2011/>, 2011.
- [Ref:27] Peters, K., Stier, P., Quaas, J., and Graf, H.: Aerosol indirect effects from shipping emissions: sensitivity studies with the global aerosol-climate model ECHAM5-HAM, *Atmospheric Chemistry and Physics*, 12, 5985–6007, doi:10.5194/acp-12-5985-2012, <http://www.atmos-chem-phys.net/12/5985/2012/>, 2012.
- [Ref:28] Roeckner, E., Bäuml, G., Bonaventura, L., Brokopf, R., Esch, M., Giorgetta, M., Hagemann, S., Kirchner, I., Kornbluh, L., Manzini, E., Rhodin, A., Schlese, U., Schulzweida, U., and Tompkins, A.: The atmospheric general circulation model ECHAM5, part I: model description, Tech. Rep. 349, Max Planck Institute for Meteorology, Hamburg, 2003.
- [Ref:29] Roeckner, E., Rospok, R. B., Sch, M. E., Giorgetta, M. G., and Hagemann, S. H.: Sensitivity of Simulated Climate to Horizontal and Vertical Resolution in the ECHAM5 Atmosphere Model, *Journal of Climate*, 19, 3771–3791, 2006.
- [Ref:30] Roelofs, G. J., Stier, P., Feichter, J., Vignati, E., and Wilson, J.: Aerosol activation and cloud processing in the global aerosol-climate model ECHAM5-HAM, *Atmospheric Chemistry and Physics*, 6, 519–548, doi:10.5194/acpd-6-519-2006, <http://www.atmos-chem-phys-discuss.net/6/519/2006/>, 2006.
- [Ref:31] Stier, P., Feichter, J., Kinne, S., Kloster, S., Vignati, E., Wilson, J., Ganzeveld, L., Tegen, I., and Werner, M.: The aerosol-climate model ECHAM5-HAM, *Atmospheric Chemistry and Physics*, 5, 1125–1156, 2005.
- [Ref:32] Stier, P., Feichter, J., Kloster, S., Vignati, E., and Wilson, J.: Emission-Induced Nonlinearities in the Global Aerosol System : Results from the ECHAM5-HAM Aerosol-Climate model, *Journal of Climate*, 19, 3845–3862, 2006a.
- [Ref:33] Stier, P., Feichter, J., Roeckner, E., Kloster, S., and Esch, M.: The evolution of the global aerosol system in a transient climate simulation from 1860 to 2100, *Atmospheric Chemistry and Physics*, 6, 3059–3076, doi:10.5194/acp-6-3059-2006, <http://www.atmos-chem-phys.net/6/3059/2006/>, 2006b.
- [Ref:12] Stier, P., Seinfeld, J. H., Kinne, S., and Boucher, O.: Aerosol absorption and radiative forcing, *Atmospheric Chemistry and Physics*, 7, 5237–5261, 2007. Stier, P., Schutgens, N. A. J., Bellouin, N., Bian, H., Boucher,
- [Ref:13] O., Chin, M., Ghan, S., Huneeus, N., Kinne, S., Lin, G., Ma, X., Myhre, G., Penner, J. E., Randles, C. a., Samset, B., Schulz, M., Takemura, T., Yu, F., Yu, H., and Zhou, C.: Host model uncertainties in aerosol radiative forcing estimates: results from the AeroCom Prescribed intercomparison study, *Atmospheric Chemistry and Physics*, 13, 3245–3270, doi:10.5194/acp-13-3245-2013, <http://www.atmos-chem-phys.net/13/3245/2013/>, 2013
- [Ref:14] Timmreck, C., Graf, H.-F., Lorenz, S. J., Niemeier, U., Zanchettin, D., Matei, D., Jungclaus, J. H., and Crowley, T. J.: Aerosol size confines climate response to volcanic super-eruptions, *Geophysical Research Letters*, 37, doi:10.1029/2010GL045464, <http://doi.wiley.com/10.1029/2010GL045464>, 2010.

- [Ref:15] Vignati, E., Wilson, J., and Stier, P.: M7: An efficient size-resolved aerosol microphysics module for large-scale aerosol transport models, *Journal of Geophysical Research*, 109, D22202, doi:10.1029/2003JD004485, <http://doi.wiley.com/10.1029/2003JD004485>, 2004.
- [Ref:16] Zhang, K., O'Donnell, D., Kazil, J., Stier, P., Kinne, S., Lohmann, U., Ferrachat, S., Croft, B., Quaas, J., Wan, H., Rast, S., and Feichter, J.: The global aerosol-climate model ECHAM-HAM, version 2: sensitivity to improvements in process representations, *Atmospheric Chemistry and Physics*, 12, 8911–8949, doi:10.5194/acp-12-8911-2012, <http://www.atmos-chem-phys.net/12/8911/2012/>, 2012.



**RAL Space**  
STFC Rutherford Appleton Laboratory,  
Harwell Oxford,  
Didcot,  
OX11 0QX UK  
[www.stfc.ac.uk/RALSpace](http://www.stfc.ac.uk/RALSpace)

Document: Final Report

Customer Ref: ITT 13/207655

RAL Space Ref: SSTD1628

2015-08-24

Page **66** of **66**